Molecular Microbiology (2014) 92(5), 1072–1091 ■
doi:10.1111/mmi.12614
First published online 2 May 2014

CRP represses the CRISPR/Cas system in *Escherichia coli*: evidence that endogenous CRISPR spacers impede phage P1 replication

Chi-Dung Yang,[1] Yen-Hua Chen,[1†] Hsi-Yuan Huang,[1,2] Hsien-Da Huang[1,2] and Ching-Ping Tseng[1*]
[1]*Department of Biological Science and Technology, National Chiao Tung University, Hsin-Chu 300, Taiwan.*
[2]*Institute of Bioinformatics and Systems Biology, National Chiao Tung University, Hsin-Chu 300, Taiwan.*

Summary

The CRISPR/Cas system is an important aspect in bacterial immunology. The anti-phage activity of the CRISPR system has been established using synthetic CRISPR spacers, but *in vivo* studies of endogenous CRISPR spacers are relatively scarce. Here, we showed that bacteriophage P1 titre in *Escherichia coli* decreased in the glucose-containing medium compared with that in the absence of glucose. This glucose effect of *E. coli* against phage P1 infection disappeared in *cse3* deletion mutants. The effect on the susceptibility to phage P1 was associated with cAMP receptor protein (CRP)-mediated repression of *cas* genes transcription and crRNA maturation. Analysis of the regulatory element in the *cse1* promoter region revealed a novel CRP binding site, which overlapped with a LeuO binding site. Furthermore, the limited sequence identity between endogenous spacers and the phage P1 genome was necessary and sufficient for CRISPR-mediated repression of phage P1 replication. *Trans*-expression of the third and seventh spacers in the CRISPR I region or third and sixth spacers in the CRISPR II region effectively reduced phage P1 titres in the CRISPR deletion mutants. These results demonstrate a novel regulatory mechanism for *cas* repression by CRP and provide evidence that endogenous spacers can repress phage P1 replication in *E. coli*.

Accepted 9 April, 2014. *For correspondence. E-mail cpts@cc.nctu.edu.tw; Tel. (+886) 3 5712121 ext. 56908; Fax (+886) 3 5729288. †Present address: Department of Microbiology and Immunology, Columbia University, New York, NY 10032, USA.

Introduction

Clustered regularly interspaced short palindromic repeats (CRISPRs) are part of an adaptive immune system in diverse bacteria and archaea (Wiedenheft *et al.*, 2012). Two CRISPR elements, CRISPR I and CRISPR II, have been defined in the *Escherichia coli* genome (Touchon *et al.*, 2011). The CRISPR I element is located downstream of eight *cas* genes (*cas1*, *cas2*, *cas3*, cse1, *cse2*, *cse4*, *cas5e* and *cse3*) (Makarova *et al.*, 2011). The latter five genes encode proteins required for forming a CRISPR-associated complex for antiviral defence (Cascade). By contrast, no *cas* gene has been found around the CRISPR II element (Diez-Villasenor *et al.*, 2010; Pougach *et al.*, 2010).

Each *cas* gene plays a distinct role in *E. coli*. The genes *cas1* and *cas2* add new spacers into the CRISPR region near the leader sequence (Yosef *et al.*, 2012). This mechanism provides the host with an immunological memory for distinguishing invading DNA molecules. CRISPR/Cas immunity system in *E. coli* involves a hierarchical process, in which CRISPR elements are transcribed into an RNA precursor (pre-crRNA) and then processed by Cse3, an RNA endonuclease, to form mature crRNAs. Subsequently, these crRNAs remain bound to Cse3 proteins and are loaded into Cascade complexes (Brouns *et al.*, 2008). The Cascade–crRNA complex binds to negatively supercoiled foreign DNA, such as a plasmid or phage DNA genome, leading CRISPR-associated endonuclease Cas3 recruitment for DNA degradation (Westra *et al.*, 2012). The *E. coli*-subtype CRISPR/Cas system reportedly targets double-stranded DNA, but recent studies have demonstrated that the Cmr-subtype Cas protein complex from *Pyrococcus furiosus* cleaves single-stranded RNA, whereas that from *Streptococcus thermophilus* cleaves double-stranded DNA (Hale *et al.*, 2008; Garneau *et al.*, 2010).

The *cas* genes expression in *E. coli* K12 is activated by LeuO but repressed by heat-stable nucleoid-structuring protein (H-NS) (Pul *et al.*, 2010; Westra *et al.*, 2010). LeuO, a LysR-type transcription factor, belongs to the helix–turn–helix-type transcriptional regulator (Henikoff

et al., 1988; Ueguchi *et al*., 1998), whereas H-NS, a dominant histone-like protein, is expressed during exponential growth (Ali Azam *et al*., 1999). The low LeuO expression level and relatively abundant H-NS result in limited CRISPR/Cas system activity (Westra *et al*., 2010). Artificial introduction of perfectly matched spacers into the CRISPR loci provides resistance against phage (Brouns *et al*., 2008), but the potential immunological function of endogenous spacers remains unclear.

Glucose is one of the major carbon sources of *E. coli*. In response to glucose availability in the environment, *E. coli* has developed a sophisticated regulatory system that effectively allocates energy and switches between alternative carbon sources (Thattai and Shraiman, 2003). For glucose metabolism, *E. coli* produces pleiotropic regulators of gene regulation, such as cyclic AMP (cAMP) and cAMP receptor protein (CRP), which form a complex (cAMP–CRP) (Kolb *et al*., 1993). This complex plays a central role in the transcriptional regulation of carbohydrate metabolism (Kolb *et al*., 1993). Recently, we observed that the bacteriophage P1 replication ability inside susceptible *E. coli* K12 was reduced in the Luria–Bertani (LB) medium containing glucose (40 mM) in compared with host cells grown in LB medium alone, and this effect was associated with a low glucose-induced, cAMP-repression of *cas* expression.

The *E. coli* CRISPR system is involved in phage defence (Barrangou *et al*., 2007; Deveau *et al*., 2010; Westra and Brouns, 2012). Using a strain with a synthetic CRISPR cassette carrying a λ-specific spacer, Pougach *et al*. demonstrated that λ phage development is inhibited in wild-type cells and prevented in an *hns* deletion mutant (Pougach *et al*., 2010). However, most functional studies on the CRISPR system in bacteria used artificial or perfectly matched CRISPR spacers against phages to demonstrate immune functions of such systems. Functional studies on endogenous CRISPR spacers are lacking.

In this study, we explored the connection between CRISPR/Cas system activity and carbohydrate availability. We demonstrated that glucose significantly enhances anti-phage P1 activity by increasing the mRNA expression of *cas* genes. We elucidated the effects of cAMP–CRP regulation on *cas* genes and CRISPR through *in vivo* and *in vitro* experiments.

We also clearly demonstrated that mutants lacking *cse3* or CRISPR elements are more susceptible to phage P1 infection. To understand why the CRISPR/Cas system specifically impedes P1 replication, we further characterized the effect of CRISPR spacers on immune responses to phage P1 infection. Our findings indicate that phage P1 replication increased in mutants with a defect in the CRISPR system, whereas *trans*-expression of endogenous CRISPR spacers recognizing the phage P1 genome reduced phage titre in the CRISPR deletion mutants. Efficiency of spacers with imperfect matches to target DNA molecules is positively correlated with the degree of sequence homology. Furthermore, flexibility of target recognition is greater than that reported previously (Semenova *et al*., 2011). Thus, endogenous spacers can repress phage P1 replication despite imperfect matching sequences. The results of this study provide comprehensive experimental evidence that CRP represses *cas* genes and provides the first direct evidence that endogenous spacers repress phage P1 replication in *E. coli* K12 by imperfect sequence matches.

Results

The CRISPR/Cas system in E. coli *K12 reduced phage P1 titre by the glucose effect*

Incorporation of synthetic CRISPR spacers matching the λ or M13 phage provide *E. coli* with immunity against those phages (Brouns *et al*., 2008; Semenova *et al*., 2011), but whether endogenous CRISPR spacers are involved in anti-phage immunity is unclear. The bacteriophage plaque assay demonstrates the ability of bacteriophages to replicate inside a susceptible host cell by measuring plaque-forming units (PFUs) (Brouns *et al*., 2008). In this study, PFUs of bacteriophage P1 in *E. coli* K12 were reduced in LB medium containing glucose (40 mM) in compared with host cells grown in LB medium alone (Fig. 1A). To determine whether this effect was restricted to phage P1, we monitored the replication rates of several common *E. coli* phages with different life cycles and genetic compositions, including P1, λ, T4, T5, T7 and ΦX147.

According to genetic composition, the tested phages can be divided into two major groups. Group I phages are double-stranded DNA viruses, including P1, λ, T4, T5 and T7 phages, and can be subdivided into temperate and lytic phages. P1 and λ are temperate bacteriophages with different lysogenic cycles. When undergoing a lysogenic cycle, the phage P1 genome exists as a plasmid and does not integrate into the host DNA, whereas the λ phage can reside within the genome of its host through lysogeny. In contrast, T4, T5 and T7 can only undergo a lytic life cycle. The group II phage ΦX174 has a single-stranded DNA genome. The plaque assay revealed that glucose in the medium selectively reduced phage P1 titre (Fig. 1A), which suggests that glucose-regulated immunity is phage P1 specific. The CRISPR/Cas system in *E. coli* functions as an immune system that depends on CRISPR RNA-guided DNA recognition (Brouns *et al*., 2008). We hypothesized that this system may participate in glucose-mediated enhancement of anti-phage P1 immunity.

To determine whether the CRISPR/Cas system was responsible for anti-phage P1 immunity, we monitored

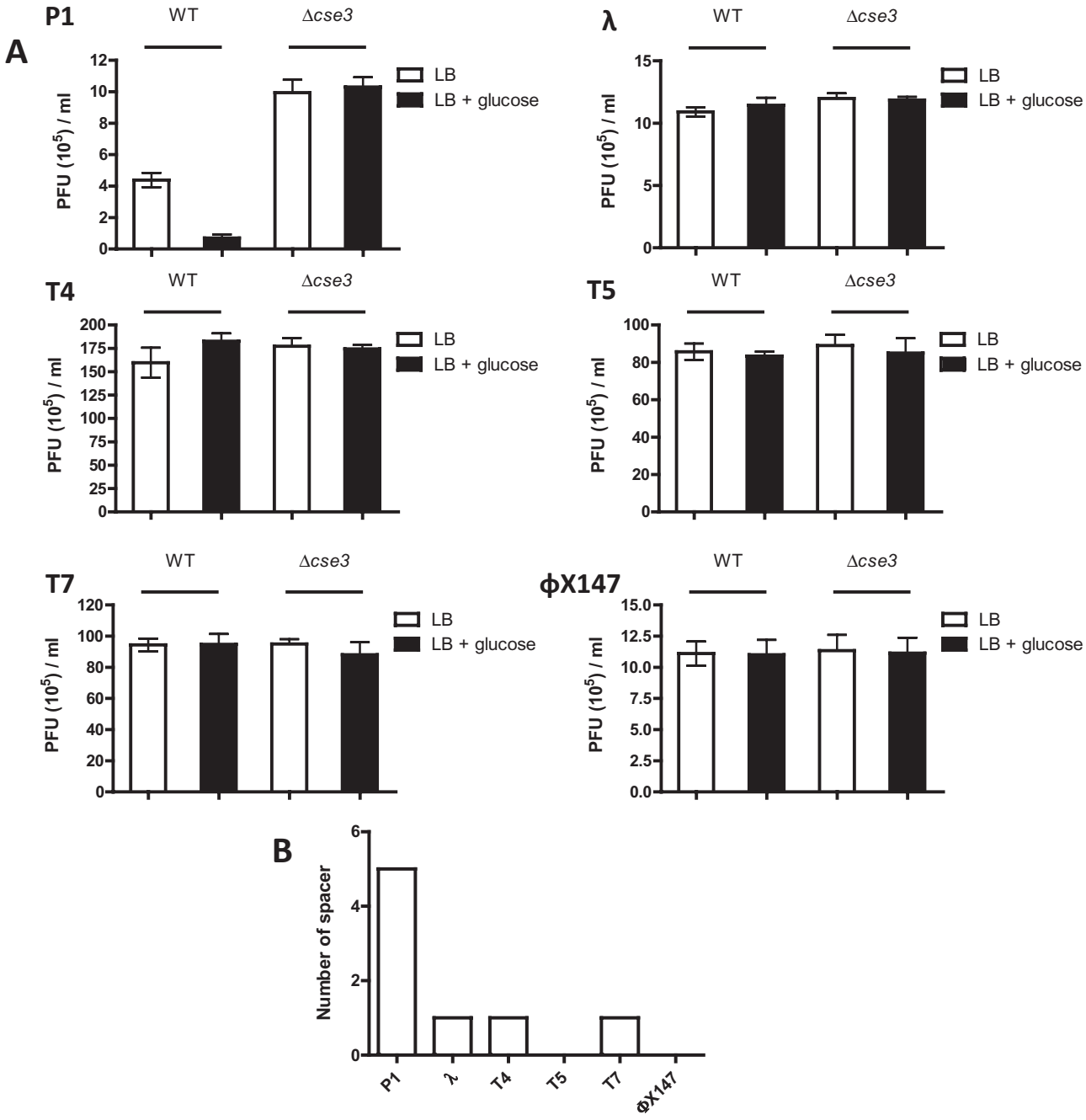

Fig. 1. Susceptibility of *E. coli* against different phages.
A. Bacteriophages (10^5 PFU: plaque-forming units) were incubated with either wild-type (WT) or *cse3* deletion mutant in the absence or presence of glucose (40 mM). The mixture was incubated at 37°C for 15 min and then lysed by adding 200 μl chloroform. Susceptibility was calculated by infecting fresh WT strain with the phage solution collected from each test group and comparing the phage titres (PFU ml^{-1}). Each data point was repeated thrice, and data are shown as means ± SEM.
B. Distribution of protospacers in *E. coli*. The bar charts illustrate the number of *E. coli* spacers in the CRISPR database that were found to base pair with different phage genomes for more than 15 base pairs, which is half the size of the *E. coli*-type CRISPR.

differences in phage P1 replication rates in the wild-type *E. coli* K12 strain and its derivative *cse3* deletion mutant, which cannot produce crRNA and lacks CRISPR/Cas-mediated immunity (Brouns *et al.*, 2008). The plaque assay showed that *cse3* deletion mutation results in three-fold increase in the phage P1 titre (Fig. 1A), suggesting that the CRISPR/Cas system may limit phage P1 replication. Furthermore, the *cse3* deletion mutation also abol-

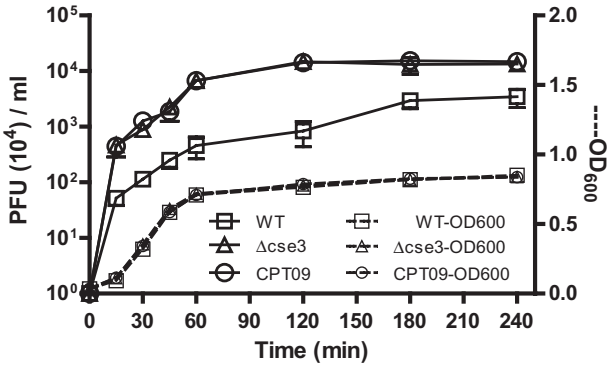

Fig. 2. One-step growth curves of the phage P1 grown on *E. coli* wild-type, *cse3* deletion mutant, and CRISPR I-CRISPR II double deletion mutant (CTP09) in LB medium without glucose. Phage titres of cell lysate from WT strains (□), CRISPR I-CRISPR II double deletion mutant (CTP09) (○), and *cse3* deletion mutant (△). Each data point was repeated thrice, and data are shown as mean value.

ished the glucose effect of *E. coli* K12 against phage P1 infection. These results hinted that glucose effects may be associated with CRISPR/Cas system regulation.

The specificity of CRISPR/Cas system depends on the sequence of CRISPR spacers. We used the BLASTn program (downloaded from National Center for Biotechnology Information, NCBI) to determine the similarity between *E. coli* K12 CRISPR spacers and genomes of the phages used in the plaque assay. Bar charts in Fig. 1B illustrate the abundance of CRISPR spacers, which can be base paired with the phage sequence spanning at least 15 in 32 nucleotides of the *E. coli* K12 CRISPR spacer (Fig. 1B). In agreement with the susceptibility against different phages, *E. coli* K12 CRISPER regions are enriched with potential CRISPR spacers against P1 phage, but very few spacers against other selected phages.

The growth kinetics of phage P1 in wild-type cells was compared with that in the *cse3* deletion and CRISPR I–CRISPR II double-deletion mutants using one-step growth curve technique in LB medium alone (Ellis and Delbruck, 1939). The curves showed that the yield of phage P1 was 10-fold higher in the *cse3* or CRISPR deletion mutant cells than in the wild-type cells after infection with phage for 60 to 120 min (Fig. 2). The *cse3* deletion and CRISPR I–CRISPR II double-deletion mutants had the same effect in controlling phage titres, and thus, the anti-phage P1 activity may require crRNA processing and expression. However, when the incubation time was extended to 240 min, the difference between phage titres in the wild type and deletion mutant strains decreased to twofold. The CRISPR/Cas system of *E. coli* K12 can retard the phage P1 replication rate but cannot completely protect *E. coli* K12 from phage P1 infection.

Susceptibility of phage P1-infected hosts in medium containing glucose is associated with LeuO but independent of H-NS

The above results established that the susceptibility of *E. coli* K12 to phage P1 decreased in the presence of glucose and that the glucose effect of *E. coli* K12 against phage P1 infection was absent in the *cse3* deletion mutants (Fig. 1). We explored the regulatory mechanism of such a phenomenon. LeuO activates expression of the CRISPR/Cas system in *E. coli* K12, whereas H-NS shows the opposite effect (Westra *et al.*, 2010). To clarify whether these transcription factors are associated with the observed glucose effect, we compared phage titres in the wild-type, and *cse3*, *hns* and *leuO* deletion mutants in the LB medium with or without glucose (Fig. 3). The increased phage titres in the *cse3* and *leuO* deletion mutants were comparable, which suggests that transcriptional activation of the CRISPR/Cas system depends on LeuO activator activity, consistent with findings from a previous study (Westra *et al.*, 2010). In contrast, the phage titre in the *hns* deletion mutants was further reduced by glucose addition, indicating that H-NS is not the only repressor mediating the glucose effect. This finding suggests the presence of an additional regulatory mechanism controlling the glucose effect of *E. coli* K12 against phage P1 infection.

cas transcription is negatively regulated by the cAMP–CRP complex

To rule out the indirect mediation of the glucose effect on *cse1* gene regulation by H-NS and LeuO, and to determine

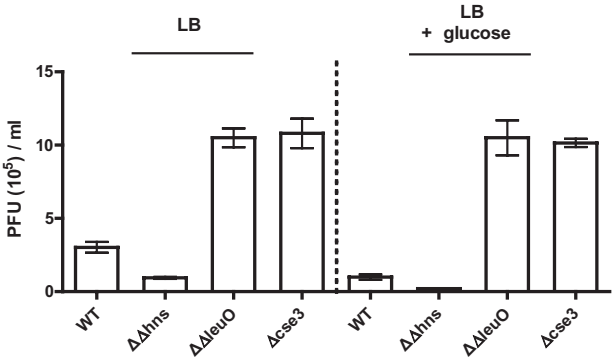

Fig. 3. Susceptibility of *E. coli* wild-type and mutant strains against P1 phages in the presence or absence of glucose in LB broth. All strains were grown in the presence or absence of glucose in LB broth supplied with glucose (40 mM) to decrease the intracellular cAMP level. The culture conditions are denoted above the columns, and the strains used in each experiment are indicated at the bottom of each column. The susceptibility of the P1 infection was characterized by the number of phage titres in the cell lysate (PFU ml^{-1}). The addition of glucose (40 mM) decreased the intracellular cAMP level, and thus alleviated CRP repression.

whether environmental glucose concentrations regulate H-NS and LeuO transcription, we analysed the relative expression levels of both genes in the presence and absence of glucose using real-time PCR. The abundance of *hns* and *leuO* mRNAs remained the same in the presence and absence of glucose (Fig. S1A and B), which suggests that novel regulators are involved in the glucose effect.

CRP is a well-known transcription factor governing carbohydrate metabolism (Kolb *et al*., 1993). When *E. coli* grows in a medium containing glucose, intracellular cAMP concentrations are low (Lawson *et al*., 2004). To investigate whether the glucose effect on CRISPR/Cas system activity is associated with CRP, real-time PCR was performed to measure mRNA expression of the *cas* operon, which encodes most components of the Cascade complex, in the wild type and *crp* deletion mutant cells. We found that the abundance of the *cse1* transcript increased threefold in the presence of glucose and was positively correlated with glucose concentrations (Fig. 4A). In the *crp* deletion mutant cells, *cse1* expression was not altered by changing glucose concentration in the medium. This result suggests that CRP is a mediator linking glucose concentration with *cse1* expression and that expression is not caused by the indirect effects of high glucose concentration in the medium. The glucose effect on *cse1* can also be observed in *hns* deletion mutants but not in the *crp–hns* double-deletion mutants, indicating that *crp*, rather than *hns*, mediates the glucose effect on CRISPR/Cas system activity (Fig. 4A). Furthermore, we excluded the possibility that CRP regulates *leuO* and *hns* expression by comparing their mRNA levels in the wild type and *crp* deletion mutant cells using real-time PCR (Fig. S1C).

The DNA-binding ability of CRP is regulated by cAMP concentrations (Kolb *et al*., 1993; Blaszczyk *et al*., 2001). Therefore, we determined whether CRP can regulate *cas* operon expression under different cAMP concentrations (0 mM to 10 mM). A quantitative measurement of CRP-mediated transcriptional regulation was performed by measuring the *cas* genes expression level in an *E. coli* K12 strain lacking the *cyaA* gene, which produces endogenous cAMP (Aiba *et al*., 1984), under different cAMP concentrations. mRNA levels of most *cas* genes decreased by 50% to 80% in LB medium with cAMP at 3 mM, but no significant reduction was observed in the *cas3* mRNA level, which is not regulated by the *cse1* promoter (Westra *et al*., 2010) (Fig. 4B). We further measured the *cse1* expression level in the *cyaA–hns* double-deletion mutants under different cAMP concentrations. Increasing cAMP concentrations in the medium reduced the *cse1* mRNA level in the *hns* deletion mutants, but not in the *crp–hns* double-deletion mutants (Fig. S1D). This result reiterates that CRP-mediated repression of the *cse1* operon is H-NS independ-

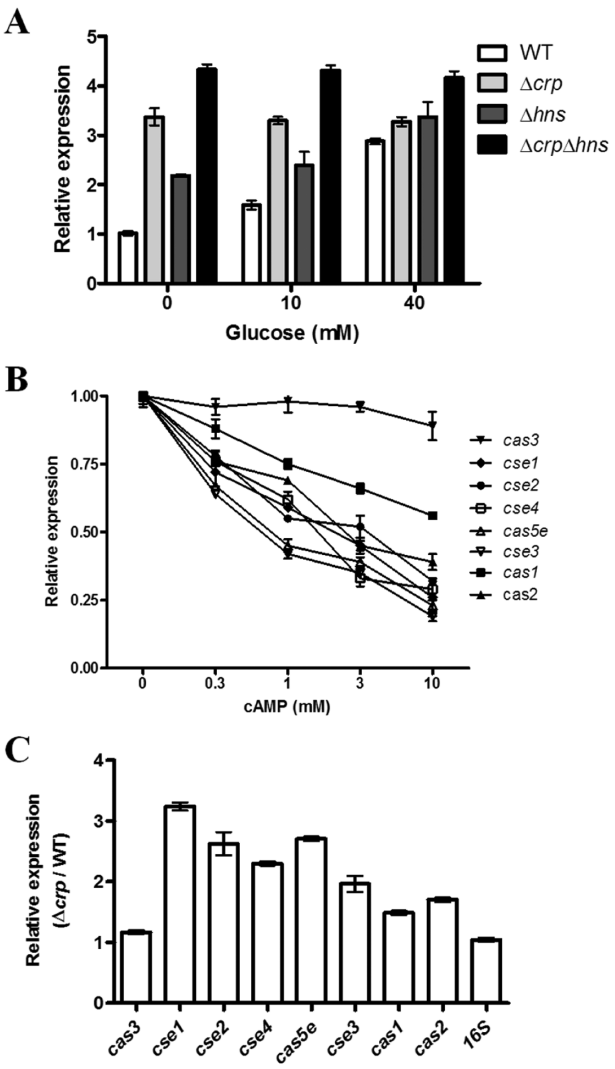

Fig. 4. cAMP–CRP complex regulates *cas* gene expression.
A. Effect of glucose concentration on *cse1* gene expression in WT and its derivatives' *crp* deletion, *hns* deletion and *crp hns* double deletion mutants (Δ*crp*, Δ*hns* and Δ*crp*Δ*hns*). All *E. coli* strains were grown in an LB medium containing glucose. Relative *cse1* expression in all strains was measured by real-time PCR (in triplicate). Bar charts illustrate the relative *cse1* expression in the LB broth with different glucose concentrations. *cse1* expression in the absence of glucose in WT was set to one.
B. The expression of *cas* operon in *E. coli* was cAMP-dose-dependent. The *cyaA* deletion mutant, which neither synthesized endogenous cAMP nor released intracellular cAMP, was grown within the LB medium containing glucose (40 mM) and incubated until OD_{600} reached 0.45. The cells were then exposed to different cAMP concentrations for 15 min. mRNA expression of *cas* genes were measured by real-time PCR (in triplicate).
C. Expression profiles of the *cas* genes in the *crp* deletion mutant (Δ*crp*). WT and *crp* deletion mutants (Δ*crp*) were cultured in LB with cAMP (1mM) to fully activate CRP until OD_{600} reached 0.45. The effect of CRP on the transcriptional expression of the *cas* gene cluster was analysed by real-time PCR (in triplicate). For all experiments, the relative gene expression level of the 16S rRNA of each RNA sample was used as an internal control to normalize gene expression.

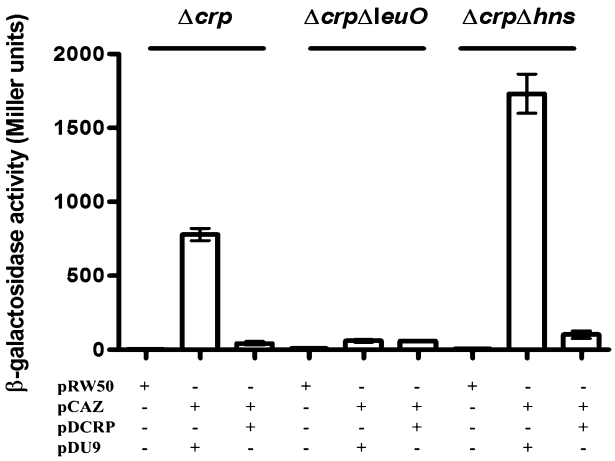

Fig. 5. CRP represses the *cse1* promoter expression of *cse1*::*lacZ* reporter fusion. The bar charts illustrate the measured β-galactosidase activities in WT derivatives' *crp* deletion, *crp leuO* double deletion and *crp hns* double deletion mutants (Δ*crp*, Δ*crp*Δ*leuO* and Δ*crp*Δ*hns*) transformed with either pCAZ, a reporter plasmid that encompasses the promoter fragment of *cse1*, or pRW50 (Empty Vector), which lacks the *cse1* promoter fragment and serves as a control. The pDCRP (CRP-expression plasmid)-encoding WT CRP was used to recover the intracellular CRP level. The empty pDU9 vector serves as a negative control.

ent. In contrast, in the *crp* deletion mutant cells, transcription of all *cas* genes except *cas3* increased compared with the transcription level in the wild-type cells (Fig. 4C). Expression levels of these genes (*cse1BCDE* and *cas1* and *cas2*) decreased with increasing distance from the transcription start site of the *cse1* promoter. A similar effect was also reported for the LeuO-mediated regulation of *cas* genes (Westra *et al*., 2010). These results suggest that CRP acts as a repressor of *cse1 operon*, whereas *cas3* expression is driven by an independent promoter (Westra *et al*., 2010).

Analysis of effects of the cAMP–CRP complex and LeuO on cse1 promoter activity

To investigate the effect of CRP, LeuO and H-NS on *cse1* promoter activity in *E. coli* K12, we generated a plasmid pCAZ carrying a *cse1::lacZ* reporter fusion construct. cAMP–CRP complex-induced repression of the *cse1* promoter was quantified by β-galactosidase assay. With plasmid expression of the wild-type CRP in the *crp* gene deletion strain, the *cse1* promoter activity decreased by 95% compared with that in the control group carrying an empty vector, pDU9 (Fig. 5). In addition, the *cse1* promoter activity was nearly undetectable in the *crp–leuO* double-deletion mutant, which agrees with the previous finding that LeuO is the critical activator of the *cse1* promoter (Westra *et al*., 2010). In the *crp–hns* double-deletion mutant, the *cse1* promoter activity also decreased significantly with pDCRP expression compared with pDU9 expression (Fig. 5). These results supported the finding that the repression of *cse1* promoter activity by CRP was H-NS independent.

Identification of the CRP binding site in the cse1 promoter region

To identify potential CRP binding sites in the *cse1* promoter region, EMSA and footprinting analysis were performed (Zianni *et al*., 2006; Chng *et al*., 2008; Karr, 2010; Lin *et al*., 2011). EMSA was performed first to test the interactions between the cAMP–CRP complex and three sequential fragments located from –350 to –1 bp relative to the *cse1* transcription start site. The only fragment showing retarded migration by the cAMP–CRP complex was the fragment covering the –350 to –200 bp upstream region (Fig. S2). To locate the CRP binding site precisely, the *cse1* promoter region (–350 to –200 bp) was scanned using the MATCH program (Chen *et al*., 2012) to predict the location of the cAMP–CRP complex binding site. Bioinformatics analysis revealed a potential CRP binding site between –281 to –259 bp of the *cse1* gene overlapped with a LeuO binding site (–310 to –252 bp), which reportedly activates *cas* gene expression. This potential CRP binding site did not overlap with another LeuO binding site (–159 to –102 bp) or the H-NS binding site (–236 to –221 bp) in the *cse1* promoter region (Westra *et al*., 2010) (Fig. 6A). The predicted CRP binding site was further verified by EMSA. In a typical procedure, a *cse1* fragment carrying the –294 to –245 bp upstream region of the *cse1* gene was synthesized to confirm the binding ability of the cAMP–CRP complex. Retarded migrating bands became evident with increasing CRP concentrations, whereas the NCA fragment (negative control) exhibited no CRP-binding ability (Fig. 6B).

We conducted DNase I footprinting to map the CRP binding site in a *cse1* promoter fragment covering –350 to –161 bp. Comparison of the sequence patterns in the absence and presence of CRP (0.4 μM) revealed that only one protein-protected region covering the *cse1* promoter region from –282 to –257 bp was protected by CRP (Fig. 6C). Protective regions of the *cse1* promoter were approximately 30 bp long.

The activity of *cse1*:*lacZ* reporter fusion constructing a mutant CRP binding site in the *crp* deletion mutants was not repressed by the *trans*-complementation of wild-type CRP (Fig. S3A). The increase of *cse1* promoter activity indicated that LeuO remained bound to the mutant promoter fragment (Fig. S3B) and remained an activator.

cAMP–CRP complex competes with LeuO for binding to the cse1 promoter

Results of EMSA and footprinting analyses indicate that the cAMP–CRP binding site overlapped with the activator

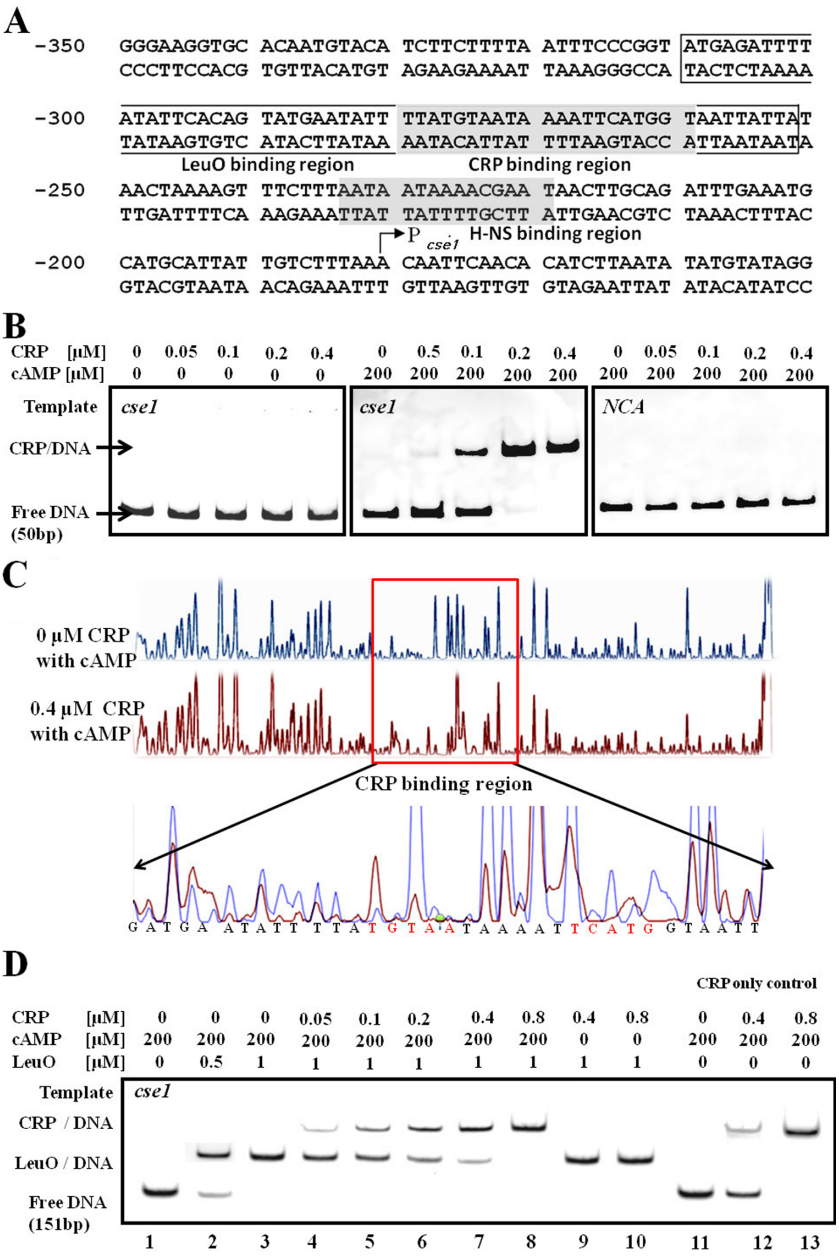

Fig. 6. Delineation of the *cse1* promoter region that interacted with the cAMP–CRP complex and its specificity.
A. Sequence of the *cse1* promoter region. The LeuO binding site is indicated by a box while the CRP and H-NS binding sites are indicated with black-shaded gray. A CRP binding site overlapped with the LeuO activator binding site. The numbers on the left denote the nucleotide positions from the transcription start site of *cse1*.
B. Binding of the cAMP–CRP complex to the *cse1* promoter *in vitro*. The DNA fragments covering the CRP binding site on the *cse1* promoter region were incubated with increasing concentrations of purified CRP protein in the presence of cAMP (200 μM) and then analysed by EMSA. The left figure shows that the CRP–cAMP complex binds to the DNA fragment carrying the predicted CRP binding sequence on the *cse1* promoter (generated by annealing synthesized nucleotides cse1-F and cse1-R). The middle picture shows the same EMSA experiment in the absence of cAMP. The picture on the right denotes the EMSA result of incubating CRP with DNA fragments containing base mutations to abolish the predicted CRP binding site (NCA fragment) and serve as a negative control.
C. DNase I footprinting assay. The figure on the top panel shows the signal in the absence of CRP, and the middle of the picture displays the signal in the presence of CRP (0.4 μM). Both reactions contain cAMP (200 μM) in a binding buffer. The figure on the bottom depicts the merged image of the upper and middle pictures around the CRP protection region.
D. CRP competes with LeuO. EMSA was conducted with purified LeuO and CRP. The cAMP (200 μM) was included in all the buffers to activate CRP binding to DNA. The *cse1* fragments (151 bp) were amplified by PCR, and then incubated with purified LeuO and CRP in an increasing concentration gradient. In the absence of CRP, LeuO binds to the *cse1* promoter fragment, causing retarded bands (lanes 1 to 3). The intensity of the retarded bands caused by the LeuO binding decreased with increasing CRP concentration, indicating that the CRP can compete with LeuO to bind to the *cse1* promoter (lanes 4 to 8). Lanes 9 and 10 show that CRP cannot compete with LeuO for the *cse1* promoter in the absence of cAMP. Lanes 11 and 13 serve as CRP only controls.

LeuO binding site. Therefore, a competition assay was conducted to verify the interaction between CRP and LeuO at the *cse1* promoter region (Fig. 6D). We initially determined whether EMSA can distinguish the retarded bands caused by LeuO and CRP. EMSA showed that the binding of the cAMP–CRP complex resulted in a slower migrating band than that of LeuO (Fig. S4). This result is compatible with the molecular weight of the cAMP–CRP complex (47 kDa) and the LeuO dimer (35 kDa) (Henikoff *et al*., 1988; Won *et al*., 2002). Subsequently, we incubated *cse1* fragments with different LeuO and CRP concentrations to determine the effect of the competition. Under constant LeuO concentrations, increasing CRP concentration reduced LeuO–DNA complexes and increased CRP–DNA complexes (Fig. 6D, lanes 3–8). However, the ability of CRP to compete with LeuO for binding the *cse1* promoter was abolished in the absence of cAMP (Fig. 6D, lanes 9–10).

The location of retarded migrating bands in the control (cAMP–CRP complex only) helped us elucidate whether the band with the lowest mobility resulted from a supershift in the presence of LeuO and CRP or CRP alone. The shifted bands in control (Fig. 6D, lanes 11–13) compared with the samples in LeuO and CRP (Fig. 6D, lanes 4–8) indicate that when CRP competed with LeuO through an overlapped binding site, LeuO lost the binding ability to the *cse1* promoter region. These results demonstrate that CRP could displace LeuO at the overlapping binding site and compete with LeuO in binding with the *cse1* promoter in the presence of cAMP.

Abundance of mature crRNA augments in crp and cyaA deletion mutants

cse3 expression level is a limiting factor for mature crRNA production (Pougach *et al*., 2010). Given this factor, northern blot analysis was performed to examine the abundance of mature crRNA. As expected, crRNA expression was nearly undetectable in the wild-type strain cultured in LB medium, whereas in the *crp* and *cyaA* deletion mutants, 60 bp bands clearly indicated a significant increase in the abundance of mature crRNA (Fig. 7), as previously seen (Westra *et al*., 2010). Likewise, increasing the glucose concentration in the medium increased the CRISPR expression. These findings indicate that CRP-mediated repression of CRISPR was reduced when extracellular glucose was abundant. Therefore, the cAMP–CRP complex not only repressed the *cas* gene expression but also limited the crRNA maturation (Fig. 7).

cAMP–CRP complex inhibits the CRISPR/Cas system in vivo

So far, we have demonstrated that CRP repressed the *cas* gene expression and negatively regulated the abundance of mature crRNA (Figs 3–7). Next, we investigated whether glucose-dependent anti-phage P1 activity was modulated by CRP through CRISPR/Cas system activity regulation. In *E. coli*, cAMP concentration is positively correlated with CRP activity (Harman, 2001). To elucidate whether the observed glucose effect was associated with intracellular cAMP concentrations and CRP activity, we investigated the effect of exogenous cAMP addition on the susceptibility to phage P1 in *crp* and *cyaA* deletion mutants. Therefore, the plaque-forming assay was performed to estimate the functions of CRP and cAMP during phage infection.

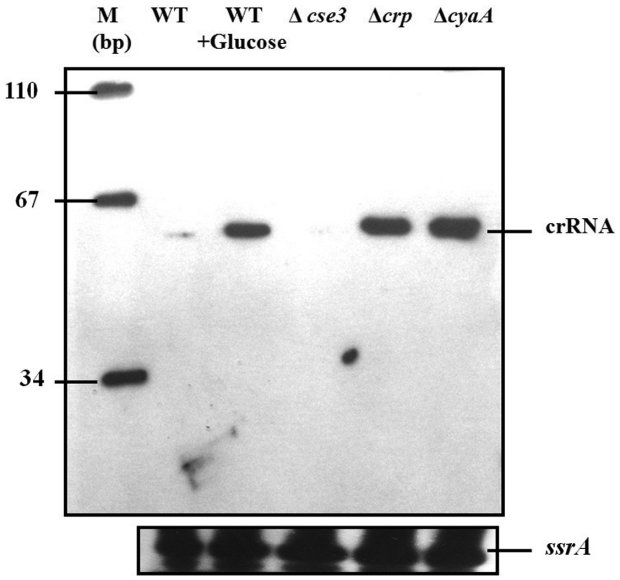

Fig. 7. Abundance of mature crRNA in the mutant strains. The levels of crRNA in WT, *cse3* deletion (Δ*cse3*), *crp* deletion (Δ*crp*) and *cyaA* deletion (Δ*cyaA*) mutants were analysed by northern blot. Similar to the effect of adding glucose (2.25 mM), the *cse3* deletion mutant (Δ*cse3*) serves as a negative control, which cannot produce crRNA and thus loses CRISPR/Cas-mediated immunity. The mRNA level of *ssrA*, which encodes the transfer-messenger RNA, serves as a loading control.

A plaque-forming assay showed that *crp* deletion strengthened the immune response of *E. coli* K12 against phage P1 infection (Fig. 8A). When cells were grown in LB broth supplemented with cAMP (1 mM), the relative PFU of the wild-type strain and *cyaA* deletion mutants increased 3.1- and 1.8-fold, respectively, compared with the cells grown in pure LB broth (Fig. 8A). Susceptibility of the *cyaA* deletion mutant cells (which do not produce cAMP) and wild-type cells, but not the *crp* deletion mutant cells, to phage P1 increased with cAMP addition. These results suggest that the glucose effect on the susceptibility to phage P1 depended on the cAMP–CRP complex.

We also investigated whether the CRP and H-NS repression effects were independent. Deletion of *hns*, which

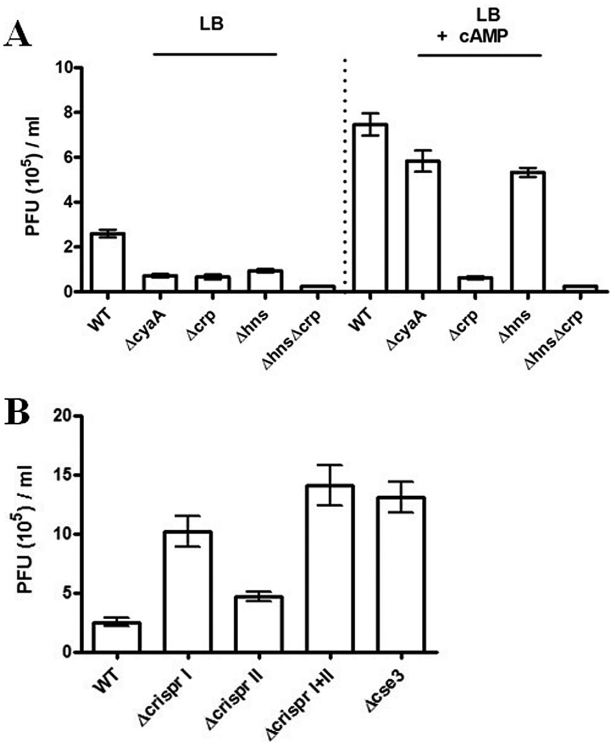

Fig. 8. Susceptibility of *E. coli* wild-type and mutant strains against P1 phages.
A. The susceptibility of the P1 infection was characterized by the phage titre in the cell lysates (PFU ml^{-1}). The addition of cAMP (10 mM) significantly increased the intracellular phage titre. The culture conditions are denoted above the columns, and the strains used in each experiment are indicated at the bottom of each column.
B. The deletion of the CRISPR I region (Δcrispr I), CRISPR II region (Δcrispr II) or CRISPR-CRISPR II double regions (Δcrispr I + II) increased the phage titres, indicating that the protection of the CRISPR/Cas system against P1 phage depended on both regions. The *cse3* deletion mutant (Δ*cse3*) strain served as an experimental control to prevent crRNA formation.

encodes a repressor of the *cse1* promoter, is sufficient to activate the anti-phage function (Westra *et al.*, 2010). Therefore, we compared the susceptibility of different mutant strains with phage P1 to determine whether CRP and H-NS operate in the same regulatory pathway. The effect of cAMP on the susceptibility to phage P1 was still observed in the *hns* deletion mutants but not in the *crp–hns* double deletion mutants (Fig. 8A). The phage titre was lower in the *crp* deletion mutant cells than in the wild-type cells, indicating that the formation of the cAMP–CRP complex was required for immune repression. Phage P1 challenge experiments, including *crp* and *cyaA* deletion mutants, helped elucidate the correlation of CRISPR activity with cAMP–CRP. To ensure the anti-phage activity mediated by CRP functions through the CRISPR/Cas system, we repeated these experiments in mutant strains with an additional *cse3* deletion mutation (Fig. S5). The results indicated that the phage P1 replication rate in the *cse3* deletion strain was independent of cAMP concentration, regardless of cAMP addition to the medium (Fig. 8A). Therefore, the metabolic regulator CRP reduced the anti-phage P1 activity by repressing the CRISPR/Cas system expression in *E. coli* K12.

Mapping the functional spacer sequence that interferes with phage P1 replication

To understand why the CRISPR/Cas system specifically reduces phage P1 titres when cultured in the medium containing glucose, we constructed different CRISPR deletion mutants and compared their susceptibilities with phage P1. The number of infectious phage particles was measured in *cse3* null and in several CRISPR deletion mutants using the plaque formation assay (Fig. 8B). The phage P1 replication rates in the *cse3* deletion and CRISPR I–CRISPR II double deletion mutants were sixfold higher than those in the wild-type strain. This result suggests that the interference of phage P1 replication was dependent on the CRISPR/Cas system. Notably, the phage titre in the cell lysate of the CRISPR I deletion mutants was higher than that of the CRISPR II deletion mutants. The higher phage titre indicates that the CRISPR I deletion mutants were more susceptible to phage P1 than the CRISPR II deletion mutant. Therefore, CRISPR I has a more important anti-phage P1 activity (Fig. 8B).

Previous studies claimed that no single genomic spacer from *E. coli* perfectly complemented any phage sequence (Pougach *et al.*, 2010). However, we found that several spacers in the CRISPR I and CRISPR II elements could be base paired with the genomic sequence of phage P1 using the BLASTn program (obtained from NCBI). Five predicted target regions in the phage P1 genome were identified (Table 1). The results indicated that CRISPR I, which is adjacent to the *cas* operon, has three spacers (spacers 3, 7 and 10) that could base pair with different regions of the phage P1 genome, whereas CRISPR II has two spacers (spacers 3 and 6) matching phage P1 genome. Among them, four spacers (3 and 7 of CRISPR I and spacers 3 and 6 of CRISPR II) form base-pairs with the phage P1 genomic sequence spanning at least 16 consecutive nucleotides.

Characterization of CRISPR spacers that target phage P1

To investigate the functional CRISPR regions that interfere with phage P1 replication, different *trans*-complementation plasmids, namely, CRISPR I (pRC1), CRISPR II (pRC2), and both regions (pRC3), were constructed and transformed into the CRISPR I–CRISPR II double deletion mutant. Similar to the results obtained in the deletion

Table 1. Predicted targets in *Enterobacter* phage P1.

CRISPR	Targeted genes	Function of targeted genes	Identities[a] (%)	Base-pairing positions[b]
Region I				
cI-3	*mlp*	Membrane lipoprotein precursor	18/22 (82%)	10–20, 24–26, 28–31
cI-7	*parA*	DNA partitioning	17/19 (90%)	14–15, 17–20, 22–32
cI-10	Non-coding	Predicted σ70 promoter of *pmgC*, a putative morphogenetic protein	15/16 (94%)	13–24, 26–28
Region II				
cII-3	*prt*	Putative portal protein	16/18 (89%)	13–17, 20–30
cII-6	*upfB*	Unknown	18/21 (86%)	1–12, 17–21

a. Indicate the number of matches/alignment length.
b. Indicate the nucleotide positions in a CRISPR spacer, which are numbered from 5′ to 3′ of each spacer.

assay, the complementation assay demonstrated that both CRISPR I and CRISPR II regions contributed to the interference effect of phage P1 replication.

The phage titres in cell lysates from CRISPR I-CRISPR II double-deletion strains (Δcrispr I + II) transformed with pRC1, pRC1 and pRC3 were lower than the phage titres in the pSP73 (empty plasmid) transformed strain, which served as the control group. This result suggests that trans-expressing CRISPR RNAs from plasmids restore the repression on phage P1 replication in CRISPR deletion strain (Fig. 9A). Immune response to phage P1 also further increased when both CRISPR I and CRISPR II regions were expressed. However, the CRISPR I spacers had a stronger anti-phage P1 effect than the CRISPR II spacers because the phage titre of pRC1-transduced strains was closer to pRC3-transduced strains than pRC2-transduced strains. These results suggest that CRISPR I and CRISPR II regions had anti-phage P1 activity.

To verify whether or not CRISPR spacers with sequences matching the P1 genome were sufficient to guide the CRISPR/Cas system to inhibit phage replication, synthesized CRISPR sequences were subcloned into the pBAD73 vector under the control of an *araBAD* promoter. We measured the level of resistance conferred by a partial match and compared it with those conferred by no match and a perfect match for each of the four spacers. The artificial plasmid have perfect match spacer can reduce the phage yield significantly. Plasmids have single native spacers slightly reduce the phage yield of host strains in comparison with the phage yield of hosts carrying a control vector (data not shown). However, the results indicated that when the two spacers that complement phage P1 on CRISPR-I or CRISPR-II coexist, substantial effects may be observed. To demonstrate that spacers with partial sequence homology to the target are also effective, we only discussed the effect of plasmids expressing two spacers in the same CRISPR region because the difference of the phage yield is more clearly (Fig. 9B).

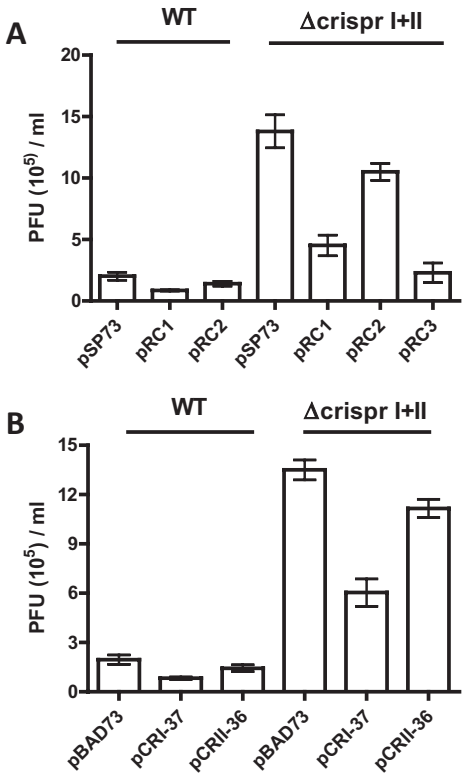

Fig. 9. Trans-complementation test confirmed the involvement of endogenous CRISPR sequence in the interference of P1 replication.
A. Different trans-complementation plasmids, namely, CRISPR I (pRC1), CRISPR II (pRC2), and both CRISPR I and CRISPR II regions (pRC3), were constructed and transformed into CRISPR I-CRISPR II double-deletion strain (Δcrispr I + II) to explore the functional CRISPR that interferes with phage P1 replication. The transformed CRISPR I-CRISPR II double-deletion strain (Δcrispr I + II) restored the repression on P1 replication in compared with the phage titre in the pSP73 (empty plasmid) transformed strain, which served as the negative control.
B. The lower panel displays the effect of the expression of the artificial CRISPR region carrying three direct repeats and two spacers under the control of the *araBAD* promoter. The cells were grown in an LB broth until OD_{600} reached 0.4, and then arabinose (5 mM) was added to induce the expression of the artificial CRISPRs. The susceptibility of P1 infection was determined by plaque-forming assay.

Each artificial CRISPR (pCRI-37 and pCRII-36) was composed of two spacer sequences (derived from the third and seventh spacers of CRISPR I or the third and sixth spacers of CRISPR II), which were interspersed by direct repeat sequences. In *trans* complementation tests, Northern blot analyses were performed to identify crRNA transcribed from the artificial CRISPR plasmids and demonstrated those crRNA mature in the CRISPR I–CRISPR II double deletion mutants (Fig. S6). The results showed that the expression of artificial CRISPR sequences that are highly similar to phage P1 genomic sequences reduced the intracellular phage titre in both the wild-type strain and CRISPR I–CRISPR II double deletion mutants (Fig. 9B). The result also showed that the combination of the third and seventh spacers from the CRISPR I region (carried by pCRI-37) imposed stronger interference on phage P1 replication than the combination of the third and sixth spacers from the CRISPR II region (carried by pCRII-36). The difference between these plasmids was more significant when using a CRISPR region double deletion mutant as a host strain. The difference between the wild-type and mutant cells suggests that endogenous crRNA co-ordinated with crRNA encoded by the plasmid to impede phage replication in wild-type strains. The artificially synthesized plasmid that contained spacers derived from the CRISPR I region provided more resistance to phage P1 infection than those from the CRISPR II region. These findings were consistent with the observed difference in the *trans*-complementation of full-length CRISPR regions. Our results suggest that endogenous CRISPR spacers imparted immunity against phage P1 infection.

CRISPR/Cas system impedes plasmid stability carrying imperfectly matched spacers

The phage P1 genome is a linear double-stranded DNA molecule in a viral particle. Once the DNA is injected into a host cell, it circularizes and replicates like a plasmid, rather than integrating into the host genome (Lobocka *et al*., 2004). A plasmid stability test was conducted to investigate whether the similarity between the CRISPR spacers and protospacers could determine the elimination rate of the foreign DNA molecule (Garneau *et al*., 2010). Therefore, we adopted the plasmid stability test to monitor how sequence similarity between crRNA and target DNA molecules affects targeted DNA molecule replication. If a sequence on a plasmid was targeted by the Cascade–crRNA complex, plasmid replication would be hindered. Therefore, when grown in a medium without antibiotics, plasmid abundance may reduce.

To determine whether the CRISPR system targets foreign DNA with imperfect matches to crRNA, four plasmids were constructed to test the replication interference of the CRISPR/Cas system. Plasmids pI3 and pI7 carried synthesized DNA fragments that matched the third and seventh spacers in the CRISPR I region respectively. Another two plasmids, pP3 and pP7, encoded a sequence that was identical with the predicted protospacers on phage P1 (Fig. 10A and Table S1). These plasmids were transformed into *E. coli* wild type and *cse3* deletion mutants that were grown in the LB medium until the optical density (OD) at 600 nm (OD_{600}) reached 1.0. Culture solution was serially diluted, spread on LB plates, and incubated at 37°C overnight. Single colonies were collected using tips and spotted on LB plates in the presence and absence of tetracycline. Antibiotic sensitivities of these colonies were inversely related with their plasmid retention ability *in vivo* (Garneau *et al*., 2010). Results also showed that the percentage of wild-type colonies that retained plasmids ranged from 35% to 63%, whereas the *cse3* deletion mutants retained all four plasmids at the same frequency (Fig. 10B). The difference in plasmid stability was clearly caused by the CRISPR/Cas system-mediated interference. The results also demonstrated that the difference in plasmid stabilities between pI3 and pI7 was $< 5\%$ in wild-type strains, whereas the difference between pP3 and pP7 was approximately 20%. This finding may be attributed to the sequence of pI3 and pI7 that perfectly matched a specific spacer, whereas pP3 and pP7 contained imperfect matches. Therefore, the stability of plasmids was inversely related to its similarity with the CRISPR spacer.

To investigate the number of base pairs required for CRISPR-mediated interference, we introduced different numbers of transversion mutations (A to T, T to A, G to C, or C to G) in pP3. The plasmid stability assay demonstrated that the introduction of two mutations increased the stability to 60%, which was significantly higher than pP3. By contrast, the introduction of four or more mutations into pP3 [pP3(d4), pP3(d6) and pP3(d9)] abolished the CRISPR-mediated interference effect (Fig. 10B). Although increasing plasmid stability by introducing two mutations in the 5′ region [pP3(5′-d2)] or the 3′ region [pP3(3′-d2)] was comparable to the effect caused by mutations on both sides [pP3(d2)], introducing two, three, or five mutations into the 5′ or 3′ complementary regions also completely abolished the CRISPR-mediated interference (Fig. S7A and B). Taken together, this evidence suggests that the target of the CRISPR system may require at least 16 bp matches with crRNA. Thus, the CRISPR/Cas system can target plasmids with imperfect matches, which is similar to the effect that can be acquired when infecting hosts with phages that carry matching sequences with host spacers. Therefore, the specificity of the *E. coli* CRISPR system against phage P1 existed because *E. coli* carried some CRISPR spacers that imperfectly matched the phage P1 genome.

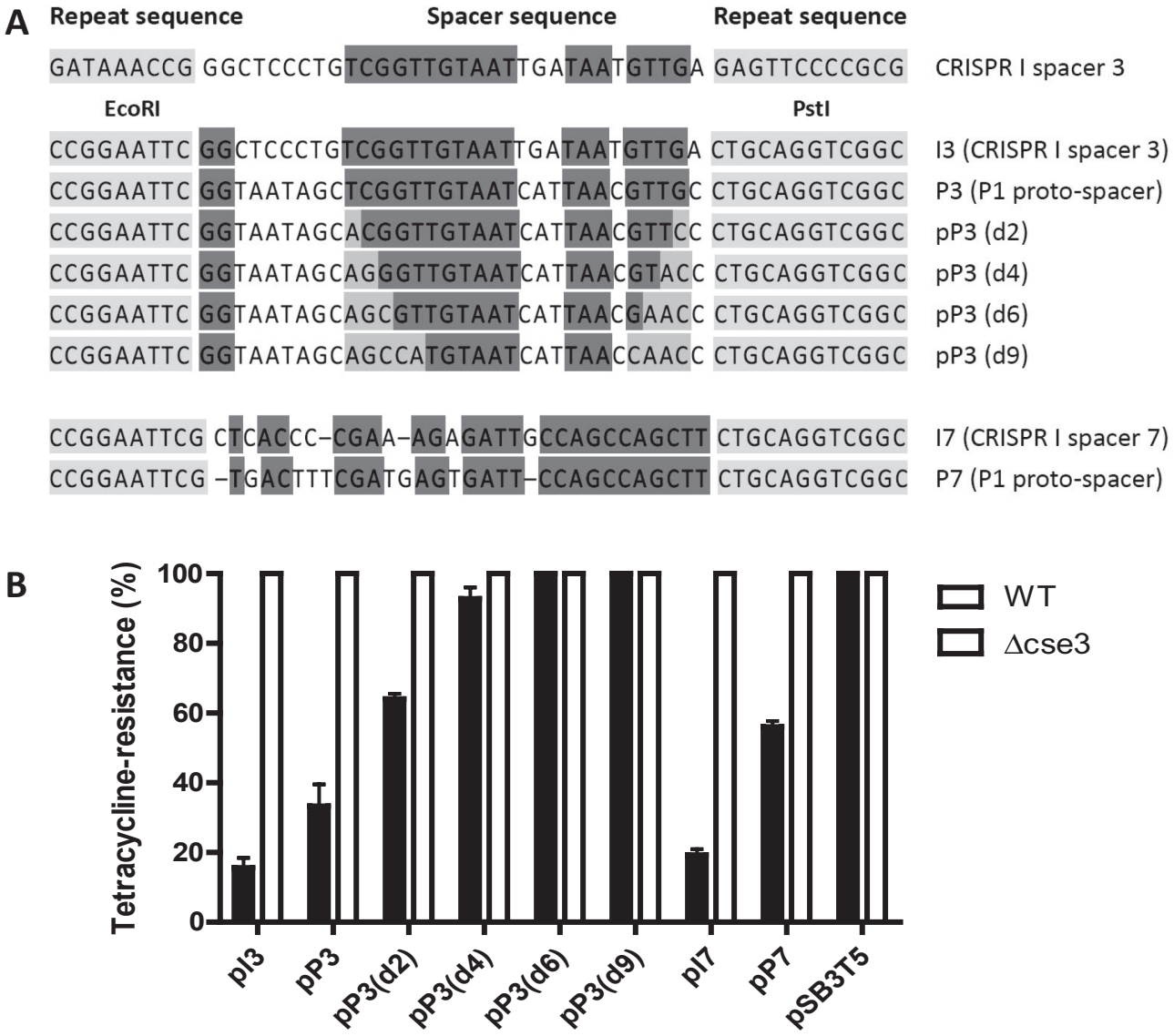

Fig. 10. Interference of a spacer on the plasmid stability is associated with the base-matched number.
A. Alignment of synthesized fragments used in plasmid stability test. Each fragment is flanked by the same adaptor sequences carrying an EcoRI cutting site at the 5′ end and a PstI site at the 3′ end. Matched bases are coloured black. The conserved region between the I3 and P3 fragments is located at the middle, whereas the most conserved regions of the I7 and P7 fragments are at their 3′ ends. The numbers of mismatched mutations in P3-derived plasmids are indicated in parentheses.
B. Transforming the WT *E. coli* strain with a plasmid pSB3T5 derivative comprising synthesized DNA fragments matching the endogenous spacers increased the elimination rate of these modified plasmids in the absence of tetracycline, whereas the parental plasmid pSB3T5 was relatively stable in the WT strain (closed bars). In the *cse3* deletion strain (Δ*cse3*), the stability of all plasmids was the same (opened bars). *E. coli* strains transformed with different tetracycline-resistant plasmids were grown in an LB medium in the absence of ampicillin until OD_{600} reached 0.8. The features of these plasmids are described in Table S2. The harvested cells were serially diluted and spread on an LB agar plate to obtain single colonies. For each test, 200 colonies were selected to test their sensitivity to tetracycline (35 μg ml^{-1}). A lower percentage of the tetracycline-resistant strains in the population results in a higher rate of plasmid elimination. A similar assay was performed in both WT and *cse3* deletion strains (Δ*cse3*).

Discussion

E. coli *represses phage P1 replication through an endogenous spacer*

Bacteria are outnumbered by the phages that infect them in different environments. To evade phage particles, bacteria have evolved various immune mechanisms, including the CRISPR/Cas system (Stern and Sorek, 2011). In this study, we analysed the mechanism by which environmental glucose concentrations affect the susceptibility of *E. coli* to phage P1. The shortage of glucose increases intracellular cAMP concentrations,

which activate CRP to repress and repressed *cse1* promoter activity. Moreover, we found that the specificity of the CRISPR/Cas system against phage P1 was provided by the pre-existing endogenous CRISPR spacers, although these spacers did not perfectly match the phage P1 genome.

In the presence of a high glucose concentration (40 mM), we found that only phage P1 had a significant reduction in PFU in wild-type strain, but this glucose effect was absent in the *cse3* deletion mutants (Fig. 1). The one-step growth curves showed that phage P1 replicated faster in *cse3* and CRISPR deletion mutants compared with those in wild-type strains (Fig. 2). Linking the two observations, the results suggested that the CRISPR/Cas system may specifically limit the replication of phage P1. The specificity of the CRISPR system against target DNA molecules is acquired from incorporating new CRISPR spacers (Marraffini and Sontheimer, 2010). A long debate exists whether the *E. coli* CRISPR system serve as an acquired immune system. Haft *et al*. (2005) claimed that the sequence analysis provides evidence that the CRISPR locus in *E. coli* may undergo degradation processes. Touchon *et al*. (2011) reported that the turnover of CRISPR spacers in *E. coli* provides little evidence to support immunity-associated diversifying selection. However, Yosef *et al*. recently demonstrated that *E. coli* can acquire new spacers when *cas1* and *cas2* are overexpressed by an inducible plasmid (Yosef *et al*., 2012). Comparing the experimental method used by Yosef *et al*. and our method, *cas1* and *cas2* transcription levels in the wild-type strain were too low and the exposure time of the bacterial cultures to the phages was relatively short. To exclude the probability that this phenomenon results from newly acquired CRISPR spacers when the *E. coli* CRISPR system is activated by glucose, we sequenced eight colonies that were randomly obtained from an *E. coli* culture infected by phage P1 with glucose for ten generations. No new spacers were found in the CRISPR region of these strains (data not shown). Taken together, our experiment design and the *E. coli* K12 strain used in this study do not prefer effectively capture new spacers. We can also rule out the possibility that the anti-phage activity observed is due to the acquisition of new spacers. In brief, the results showed that the anti-phage ability was abolished in CRISPR deletion strains and could be restored by trans-expressing specific spacers (Fig. 9A and B). Therefore, the anti-phage activity observed in this study was due to the pre-existing genomic spacers rather than the newly acquired spacers.

Repression of the CRISPR/Cas system by cAMP–CRP complex is H-NS independent

The CRISPR/Cas system is a widespread antiviral system in bacteria and archaea (Marraffini and Sontheimer, 2010). This immune system can capture pieces of DNA from phages or plasmids and integrate them into the host genome. This activity enables the bacteria or archaea to memorize the phage infection, providing the host with adaptive immunity (Brouns *et al*., 2008; Yosef *et al*., 2012). Previous studies reported that two transcription factors, LeuO and H-NS, control the expression of the CRISPR/Cas system in *E. coli* (Pul *et al*., 2010; Westra *et al*., 2010). LeuO is the activator of CRISPR/Cas transcription, and its activity is associated with ppGpp concentrations under cell stress (Fang *et al*., 2000). ppGpp concentration is hypothesized to increase during phage infection; thus, LeuO would be activated to strengthen transcription of *cas* genes (Westra *et al*., 2010). However, the hypothesis that the activity of LeuO is regulated by the production of ppGpp during phage infection was refuted because LeuO and *cas* gene expressions remained stable when *E. coli* was infected with the bacteriophage PRD1 (Poranen *et al*., 2006). Unlike LeuO, H-NS represses the CRISPR/Cas system by competing with LeuO to bind to the *cse1* promoter region (Westra *et al*., 2010). In the present study, we demonstrated that CRP also acts as a transcriptional repressor of the CRISPR/Cas system (Figs 4–7).

In summary, CRP regulation on the *cas* operon was mainly dependent on direct binding to the *cse1* promoter. CRP negatively regulates the *cse1* operon because it competes with the activator LeuO at an overlapping binding site. However, the essential binding sequence for CRP is different from that for LeuO. LeuO and CRP are both well-known global regulators that regulate genes involved in the utilization and biosynthesis of carbohydrate compounds (Keseler *et al*., 2013). Therefore, transcriptional regulation of the CRISPR/Cas system reflects the ability of *E. coli* to strategically allocate limited energy between growth and immune responses (Ueguchi *et al*., 1998; Johansson *et al*., 2000; Majumder *et al*., 2001; Gorke and Stulke, 2008). LeuO expression is induced by ppGpp and peaks when cells enter the stationary phase (Majumder *et al*., 2001), whereas the DNA-binding affinity of CRP is positively correlated with cAMP concentration (Kolb *et al*., 1993; Blaszczyk *et al*., 2001).

Based on our new findings, we propose a model of CRP-mediated regulation of the *cse1* operon. In this model, *cas* genes and the CRISPR region can be expressed only when cAMP concentrations are too low for CRP to compete with LeuO for binding to the *cas* promoter (Fig. 11). The immature pre-crRNA transcript is then processed by *cse3*, forming an interference complex that targets foreign DNA molecules. By contrast, when cAMP concentrations are augmented, such as when cells enter the stationary phase (Buettner *et al*., 1973), the DNA-binding affinity of CRP also increases, thereby allowing CRP to impede the binding of LeuO to the *cse1* promoter. Given that our study only addresses the regulatory function

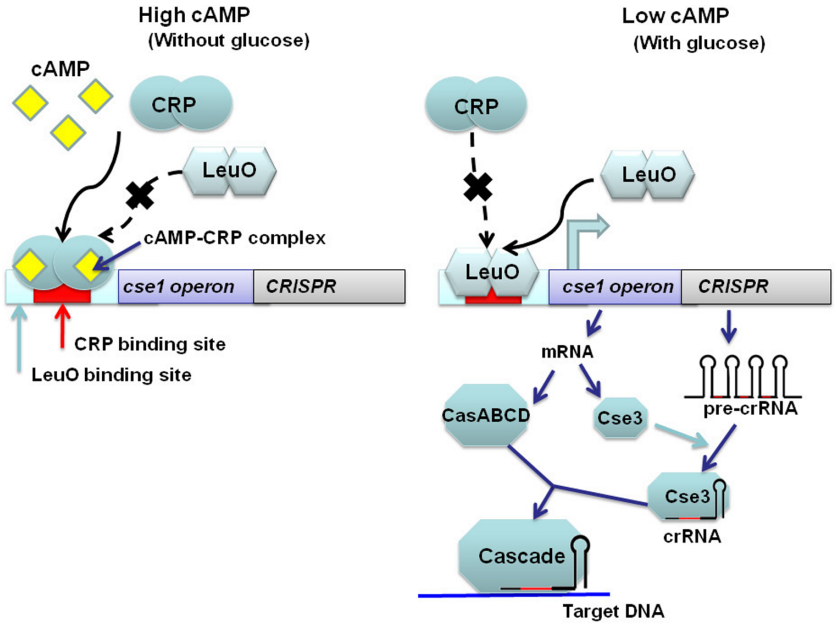

Fig. 11. Regulatory mechanism of the cAMP–CRP complex on *cse1* promoter. In LB medium without the addition of glucose, the activated adenylyl cyclase converts ATP into cAMP, which then binds to the CRP to form a cAMP–CRP complex. The complex can compete with LeuO from the *cse1* promoter region, repressing the expression of *cas* genes and CRISPR. In contrast, after the addition of glucose the cAMP levels are reduced, the limited number of activated CRP cannot compete with LeuO to bind to the *cse1* promoter, and LeuO activates the transcription of *cas* genes and precursor CRISPR RNA (pre-crRNA). This long RNA precursor was processed by the CASCADE complex and remained bound to it. The CASCADE–crRNA complex will target the DNA fragments (from P1 phage or plasmids) that can match the crRNA and recruit Cas3 (not shown), resulting in the interference. To simplify the model, this figure only includes the major plays in response to cAMP. The repression effect of *hns* on *cas* genes is not shown in this figure.

of CRP on the CRISPR/Cas system in the *E. coli* K12 BW25113. To extend our findings, we attempted to find a CRP binding site on *cse1* promoter region and the phage P1 specific CRISPR spacer in 48 *E. coli* strains with full genome sequence from NCBI, we found that there are another *E. coli* strains (e.g. *E. coli* ATCC 8739, *E. coli* BW2952, *E. coli* K12 DH10B, *E. coli* ETEC H10407, *E. coli* K12 MG1655, *E. coli* K12. W3110) have candidate CRP binding site on *cse1* promoter region and phage P1 specific CRISPR spacer (data not shown).

Therefore, we believe that our findings can be applied to other *E. coli* strains with a CRP binding site at the *cse1* promoter region and the *E. coli* type I-E CRISPR/Cas system. However, further investigation is necessary to determine whether or not this mechanism is also applicable to gamma-proteobacteria with *E. coli*-subtype *cas* gene clusters, such as *Methylococcus capsulatus*, *Photobacterium profundum* and *Salmonella* sp.

In the other hand, this is a case where cAMP and CRP positively regulate CRISPR system in *Thermus thermophilus* HB8 (Agari *et al*., 2010) . *T. thermophilus* HB8 contains several CRISPR/Cas systems. In addition to a type III-B (Cmr) and a Csx, two of these systems, type I-E and Type III-A (Csm), are shared with the *S. thermophilus* loci CRISPR4 and CRISPR2 respectively. However, CRISPR1 and CRISPR3, which are the active loci in our model organism, are idiosyncratic type II CRISPR/Cas systems; those induced by phage in the *T. thermophilus* system are type I and type III systems and have different mechanisms of action. Although this regulation contrasts our findings, but may be the activity of their phage is different or perhaps their growth environments are different.

CRISPR/Cas system targets phages or plasmids carrying imperfect matches to spacers

The CRISPR/Cas system follows a step-by-step process, where pre-mature crRNA is processed by *cse3* for maturation, and mature crRNA is then loaded into the Cascade complex (Brouns *et al*., 2008; Jore *et al*., 2011). Because the observed anti-phage activity is specific to phage P1, we expected the immune response to involve mechanisms of sequence-specific recognition, which prompted us to examine whether or not the CRISPR/Cas system involves limiting phage replication in the *E. coli* K12 strain. In this study, the one-step growth curves reflected the functional roles of the *cse3* and CRISPR regions. Phage P1 titre of the *cse3* and CRISPR deletion mutants was identical, but is significantly higher than that of wild-type strain (Fig. 8A and B). Therefore, *cse3* and CRISPR deletion mutants cannot slow down phage P1 replication.

The Cascade–crRNA complex targets DNA by base pairing between crRNA and the foreign DNA and then degrading the target DNA (Marraffini and Sontheimer, 2010). Accumulating evidence indicates that the binding of the Cascade–crRNA complex with Cas3 and DNA fragments is necessary to cause phage interference (Westra *et al*., 2012). Therefore, artificially synthesized spacers that perfectly match target DNA sequence are frequently used to study the function of Cas proteins in different bacteria strains. Although the deletion and trans-complementary assay showed that endogenous CRISPR region provided *E. coli* with specificity against phage P1 (Fig. 9), no spacers were observed that perfectly matched the genomic sequence of phage P1.

This study found that the CRISPR/Cas system could still target protospacers carrying five mismatches outside the seed region. Therefore, *E. coli* interference against phage P1 is different from the previously reported seeding model, which considered that seed sequence at the 5′ end of the CRISPR spacer is an essential marker for CRISPR/Cas system target (Semenova *et al*., 2011). By calculating the distribution of the base-pairing region of crRNA, the result showed that most of the mismatched base pairs were located at the 5′ region (Fig. S8). This phenomenon may result from the evolutional stress and adaptation of phage P1 to the CRISPR-based immune system of *E. coli*. The host with the *E. coli*-subtype CRISPR/Cas system probably encountered an ancestral phage P1 and acquired some perfectly matched spacers from the phage genome. During evolution, the CRISPR spacers remained perfectly matched with the ancestral phage P1 genome, and the most effective escape mutations accumulated in the survived phages. Thus, phage P1 accumulated sufficient mutations to overcome the defence response of *E. coli*, although its replication is still slightly affected and limited by the imperfectly matched CRISPR spacers (Fig. 9). A previous computational screening confirmed that the CRISPR region of the two *E. coli* strains (630 and ECOR44) and a plasmid of *E. coli* O111:H-11128 (EHEC) encompass a spacer (CCTGATTGATGGCTTCTTTGATGTCAAAC CGA) that perfectly complements gene *22* of the phage P1 (Mojica *et al*., 2009). Although this spacer sequence is absent in the *E. coli* BW25113 strain, we found that the numerous spacers in this strain map a region adjacent to gene *22* (covering genes *23*, *parA*, *mlp* and *upfB*) (Fig. S9). Therefore, spacers with anti-phage P1 activity may prefer to target hotspots. Several recent papers have reported the hotspots of target sites on phage and plasmid genomes (Datsenko *et al*., 2012; Paez-Espino *et al*., 2013). In addition, these spacers may also provide some flexibility to meet a broader range of phages with similar, but not identical, genomes. Wiedenheft *et al*. demonstrated that the binding affinities of crRNA reach a peak at the seeding region but decrease from the 5′ to the 3′ region of the seeding region (Wiedenheft *et al*., 2011). In addition, a proposed model claimed that a seed region composed of a 5′ protospacer-associated motif (PAM) and a perfectly matched 5′ sequence is essential for CRISPR-mediated antiviral activity (Semenova *et al*., 2011). M13 phages that accumulate some mutations in the PAM or seeding region can replicate in a host cell carrying a single CRISPR spacer that perfectly matches the M13 phage genome. Thus, these mutations are termed escape mutations (Semenova *et al*., 2011). In general, these results suggest that the CRISPR/Cas system can function through imperfect base pairing with target nucleotides in *E. coli*, similar to the microRNA system found in eukaryotic cells (Saxena *et al*., 2003; Brodersen and Voinnet, 2009). In this study, phage P1 may also be a type of phage that carries sufficient escape mutants to effectively replicate in host strains.

DNA–RNA complementary hybridization is an important part of several cellular processes. DNA–RNA hybrids are formed during general and reverse transcription, initiation of DNA replication and recombination (Lorenz *et al*., 2012). In bacteria, DNA–RNA hybrids have a function within the CRISPR pathway (Howard *et al*., 2011). We identified some spacers in the CRISPR I and the CRISPR II regions that had anti-phage P1 activity using deletion mutants and *trans*-complementation assay. Garneau *et al*. (2010) used a plasmid stability test to measure CRISPR/Cas system activity. To determine whether or not these spacers recognize phage P1 through sequence complementation as well as the minimum requirements for a spacer to impede phage replication, we conducted a plasmid stability test to evaluate whether or not the *E. coli* CRISPR system also impedes the replication of plasmids with sequence complementary to spacers. The plasmid stability test demonstrated that the higher the similarity between the plasmid sequence and spacers, the lower the stability of the plasmid (Fig. 10A and B). Therefore, the effect of the CRISPR/Cas system-mediated repression on phage and foreign DNA replication may correlate with the relative binding-free energy between crRNA transcribed from the CRISPR spacer and target DNA (Jore *et al*., 2011). A previously published EMSA experiments showed that only the sequence-matched 5′ region of the middle of crRNA can target the Cascade–crRNA complex and retard band migration (Wiedenheft *et al*., 2011). In our study, the longest base pairing region of pP3 was located at the middle of the synthesized fragment whereas that of pP7 is located at the 3′ end. Aligning the synthesized fragment of pP7 with the phage P1 genome demonstrated that an extra base bulges outside, which could destabilize the base pairing structure (Smith *et al*., 2009; Minetti *et al*., 2010). The result showed the effect of transversion mutation introduction at different positions (either closer to the 5′ or 3′ region of the spacers), but the stabilities of the derivative plasmids of pP3 suggested that the number of matches was a more important determinant of interference effect. Although the efficiency of CRISPR-mediated interference was negatively associated with the number of imperfect matches (Fig. 10 and Fig. S7), further study is required to quantitatively analyse the effect of other features, such as base bulges and the location of mismatches to better understand the elimination rate of foreign DNA species.

CRISPR loci in E. coli *K12 can target phage P1 DNA by phage P1-related sequence in the absence of conserved PAM sequences*

Earlier statistical research reported the presence of some conserved sequence patterns adjacent to the protospac-

ers, known as PAMs (Mojica *et al*., 2009). These sequence motifs are proposed to obtain new spacers and define foreign DNA sequences. Mutations in PAMs are reported to reduce, or even totally abolish, the efficiency of the anti-phage activity of the CRISPR/Cas system (Semenova *et al*., 2011). However, other studies demonstrated that the expression of a perfectly matched CRISPR sequence protected the host bacteria from specific phage infections. Despite there were no conserved ATG motif, a PAM of CRISPR/Cas systems, be found around the predicted target of phage P1 specific spacer (Brouns *et al*., 2008; Pougach *et al*., 2010). This study revealed that the CRISPR system effectively reduced plasmid stability encompassing imperfect matches to the CRISPR spacers, although the plasmids used in the stability test lacked a canonical *E. coli*-type PAM adjacent to the synthesized spacers (Fig. 10). Recent studies have provided evidence that the type I-E CRISPR/Cas system in *E. coli* K12 can target foreign DNA that can base-pair with CRISPR RNA without the conserved PAM sequence ATG. The stringency of the type I-E CRISPR/Cas system has been discussed in two independent studies (Pougach *et al*., 2010; Westra *et al*., 2013). To determine whether or not the PAM affects our observations, we constructed a plasmid with perfect complementarity and canonical PAM sequence ATG, calling it pI3-PAM. No differences were observed when we tested the effectiveness of CRISPR spacers with perfect matches using pI3-PAM (perfect complementarity and a canonical PAM sequence ATG) and pI3 (perfect complementarity and without PAM flanking one side of the protospacers) (data not shown).

The 5′ flanking sequences of most of the predicted targets of *E. coli* K12 on the phage P1 genome are not AAG, AGG, GAG and ATG, which are the PAMs usually found in the target sequences of the type I-E CRISPR/Cas system (Semenova *et al*., 2011). This finding suggests that phage P1 accumulates mutants to weaken CRISPR/Cas-mediated repression. In addition, all spacers that were found to target phage P1 genomic DNA, except the last spacer in the CRISPR II region, were also base-paired at the central region (11–28 bp). This finding suggests the reduced stringency of requirements for PAMs of *E. coli* K12 against phage P1. The evidence indicates that PAM is dispensable but may be a helpful marker in guiding the immune response.

Bacteria use the CRISPR/Cas system to capture phage DNA sequences and insert those sequences into the CRISPR loci to enhance phage resistance. By contrast, phages can break through the CRISPR/Cas-mediated defence by accumulating point mutations and deletions (Deveau *et al*., 2010). The host bacteria continuously obtain new spacers or evolve additional defensive mechanisms. Given that phages with mutations may have a high replication probability, bacteria and phage generate a selection pressure on both species, which is an important driving force for phage diversification. Previous studies provide limited data for this hypothesis because few *E. coli* spacers have been found to perfectly match the phage genomes (Mojica *et al*., 2009; Touchon *et al*., 2011). Touchon *et al*. reported that the strong correlation between multi-locus sequence types and the spacer repertoire indicates rare turnover of spacers during of *E. coli* strain diversification. Such data do not support the concept of immunity-associated diversifying selection. However, our study showed that the *E. coli* K12 BW25113 has some spacers with anti-phage P1 activities that did not perfectly match the phage DNA sequence. We also demonstrated that the expression of the two relatively conserved spacers, namely, CR1-7 and CR2-6, could impede phage P1 replication.

These results may serve as evidence that the CRISPR/Cas system in the ancestral strains of *E. coli* had actively acquired spacers from phages infecting them. Therefore, the absence of significant immune effects reported in previous studies may be explained by the accumulation of sufficient escape mutations in the tested phages (Poranen *et al*., 2006; Pougach *et al*., 2010), and because of the activity of CRISPR/cas system is limited by CRP and H-NS. Nevertheless, our results demonstrated that endogenous spacers with imperfect matches had anti-phage activity. It also suggested that this sequence-based targeting mechanism has greater flexibility than previously expected.

Experimental procedures

Bacterial strains

Mutant strains used in this study were *E. coli* BW25113 derivatives generated from the Keio collection system and were provided by the National Institute of Genetics of Japan (Baba *et al*., 2006). The features of the mutants are listed in Table S1.

Plasmid construction

The *cse1*::*lacZ* reporter plasmid, pCAZ, was constructed by introducing the PCR product with the 500 bp region upstream to *cse1* start codon into pRW50, a low-copy-number *lacZ* expression vector (provided by Dr Busby of the University of Birmingham) (Hollands *et al*., 2007). The pCAN plasmid carrying a mutant CRP binding site was derived from pCAZ by site-directed mutagenesis to verify the function of the predicted CRP binding site on the *cse1* promoter region. Three CRISPR complementary plasmids (pRC1, pRC2 and pRC3) were constructed by the insertion of CRISPR I, CRISPR II, and both regions into the pSP73 vector (Promega, Madison, WI) respectively. pBAD73 was generated by sub-cloning the *ara*BAD promoter of pBAD202/D-TOPO (Invitrogen, Carlsbad, CA, USA) into pSP73 to obtain the inducible plasmid. CRISPR complementation plasmids (pCRI-37 and pCRII-36) were constructed by cloning commercially synthesized DNA

fragments (CRI-37 and CRII-36) into the pBAD73 vector. Four pairs of synthetic oligonucleotides (I3-F/R, P3-F/R, I7-F/R and P7-F/R) were used to construct plasmids with potential CRISPR targeting sequences. Complementary single oligonucleotides were denatured at 65°C and left to cool at room temperature to allow base pairing. The double-strand DNA encompassing an EcoRI site at the 5 prime end and a PstI site at the 3 prime end was digested with restriction enzymes and subcloned into low-copy-number vector pSB3T5 (Shetty *et al.*, 2008). All primers and synthesized nucleotides used in this study are listed in Table S2.

Electrophoretic mobility shift assays

EMSAs were conducted as described in previous studies (Gaudreault *et al.*, 2009; Lin *et al.*, 2011) with some modifications. DNA fragments for EMSA were obtained by annealing commercially synthesized complementary oligonucleotides (by heating to 65°C and then cooling to room temperature) or by PCR (with primers listed in Table S2). The EMSA reaction mixtures (20 μl) contained DNA oligonucleotides (20 nM), cAMP (200 μM), and different concentrations of CRP (0, 0.05, 0.1, 0.2, 0.4 and 0.8 μM) in a buffer solution of Tris-HCl (20 mM, pH 8.0), $MgCl_2$ (10 mM), ethylenediaminetetraacetic acid (EDTA, 0.1 mM) and KCl (100 mM). The reaction mixtures were gently mixed and incubated for 30 min at 37°C to allow binding. Novel juice loading dye (GeneDireX, Las Vegas, NV, USA) was subsequently added to the reaction mixtures and separated by non-denaturing polyacrylamide gel (6%). To confirm the predicted CRP binding site on the *cse1* promoter, three fragments covering the *cse1* promoter region (from –350 to –200, –250 to –100, and –150 to –1) were synthesized by PCR (Table S2). A cse1 fragment carrying the –294 to –245 base pairs upstream of the *cse1* gene was synthesized to confirm the binding ability of the cAMP–CRP complex. The DNA fragment (NCA fragment) containing the mutated CRP binding site TTAT**C**TAATAAAATT**G**ATGGTA (a G to C mutation at position 5 and a C to G mutation at position 16) served as a negative control. To determine the competition between CRP and LeuO on the *cse1* promoter, a DNA fragment carrying –350 to –200 upstream of the *cse1* start codon was amplified by PCR and incubated with purified LeuO and CRP in the presence of cAMP (200 μM).

DNase I footprinting

DNase I footprinting assay was performed as described previously (Zianni *et al.*, 2006; Chng *et al.*, 2008; Karr, 2010; Lin *et al.*, 2011). The PCR product carrying the –350 to –161 region of the *cse1* promoter was generated by 5′FAM-labelled primers. Binding of the cAMP–CRP complex to the labelled DNA fragment was conducted as described for EMSA. The binding mixtures were then partially digested with 0.4 units DNase I (Promega, Madison, WI, USA) in the absence or presence of CRP (400 nM). After incubation for 45 s at 37°C, the reaction was stopped by heating at 98°C for 10 min without adding EDTA. The digested DNA fragments were purified using the MinElute PCR purification kit (Qiagen, Hilden, Germany) and then separated by capillary electrophoresis using the Applied Biosystems 3730 DNA analyser (Applied Biosystems, Foster City, CA, USA). The protective regions of cAMP–CRP DNA binding to DNase I digestion were analysed using the Peak Scanner Software v1.0.

Quantitative mRNA expression level

RNA manipulation and real-time PCR were performed as described previously (Lin *et al.*, 2011). RNA isolation is based on the suggested protocol in the TRI reagent-RNA kit (Molecular Research Center, Cincinnati, OH, USA). RNA samples for real-time PCR were pre-treated with DNase I (Promega, Madison, WI, USA). The DNA primers (listed in Table S2) used in real-time PCR were designed by the Primer Express software (Applied Biosystems, Foster City, CA, USA) and the complementary DNA was synthesized using Super-Script III Reverse Transcriptase (Invitrogen, Carlsbad, CA, USA). Real-time PCR was conducted by ABI PRISM® 7000 (Applied Biosystems, Foster City, CA, USA) using SYBR Premix ExTag (Takara, Tokyo, Japan). All quantitative PCR reactions were performed with six replicates.

Promoter activity assay

The activity of β-galactosidase was determined in *E. coli* BW25113-derived *crp* null strain, *E. coli* BW25113-derived *crp leuO* and *crp hns* double-deletion strains. The mutant strains were co-transformed with reporter plasmids (pCAZ and pCAN) and pDCRP, which encodes wild CRP. The pCAZ has a wild-type *cse1* promoter, whereas pCAN contains a mutation at the CRP binding site. The cells were grown in LB at 37°C until OD_{600} reached 0.4. All assays were performed with five replicates.

Northern blotting

A DNA probe specific to spacers of the CRISPR I region was commercially synthesized according to a previous study (Westra *et al.*, 2010). CRISPR probes and pUC19 DNA/MspI ladders (Fermentas, Vilnius, Lithuania) as markers were end-labelled with digoxigenin (DIG)-dUTP (Roche Applied Science, Indianapolis, IN, USA) by Terminal deoxynucleotidyl transferase in 10× TdT buffer and purified by QIAquic kit (Qiagen, Hilden, Germany). RNA samples were electrophoresed on polyacrylamide gel (8%) with urea (7 M). The separated RNA was transferred to charge the nylon membrane (Millipore, Bedford, MA, USA) using a trans-blot semi-dry transfer cell (Bio-Rad, Hercules, CA, USA). After UV-crosslink, the membrane was hybridized with specific DIG-labelled probe in FASTHyb-Hybridization solution (Biochain, Hayward, CA, USA) at 65°C for 1 h. The probed membrane was washed with DIG Wash and with the Block Buffer Set (Roche Applied Science). Finally, the anti-DIG antibody and CSPD (Roche Applied Science) were used for luminescence. The blots were exposed to X-ray films (GE Healthcare, Buckinghamshire, UK).

One-step growth curve

The experimental design is based on the method developed by Eills and Delbruck (Ellis and Delbruck, 1939). Bacterial strains were cultured in LB broth at 37°C until OD_{600} reached 0.4 and incubated with the phage solution (the ratio of bac-

teria to phage equals 100:1) at 37°C for 15 min. The bacteria were centrifuged at 3500 *g* for 10 min and washed by sterilized water. The supernatant was removed, and the pellets were resuspended in LB broth supplied with $MgSO_4$ (10 mM). The infected bacteria were grown at 37°C. The phage-cell mixtures were sampled at intervals of 0, 15, 30, 45, 60, 120, 180 and 240 min, and subsequently lysed with chloroform (1%). The number of phage particles in the cell lysate was quantified by plaque assay.

Phage plaque assay

Susceptibility of different *E. coli* strains to bacteriophages was determined by PFUs. Strains were cultured in LB broth until OD_{600} reached 0.4 and were then pretreated with glucose, cAMP, or ddH_2O for 10 min to alter the expression of *cas* genes. The pretreated cells were collected by centrifugation (3500 *g* for 10 min) and resuspended in $MgSO_4$ (10 mM). For each condition, approximately 10^8 cells were incubated with 10 μl phage solution (10^9 PFU ml^{-1}) at 37°C for 15 min), which allowed infection of host cells by the phages. Subsequently, the infected cells were lysed with chloroform (1%). The lysates were centrifuged at 13 000 *g* for 15 min and the supernatants were collected for the plaque-forming assay. The lysate was serially diluted and incubated with wild-type strain (grown in LB until OD_{600} reached 0.4) at 37°C for 15 min. The cells were mixed with top agar (3 ml) and poured on LB agar plates at 37°C for 8 h, after which plaque formation was counted.

Majority of the phage-induced changes occur only after the synthesis of virion components, indicating that no major reprogramming of host gene regulation exists during early infection (Poranen *et al.*, 2006). In general, phage strains with a higher adsorption rate have a shorter optimal lysis time and *vice versa*. For example, the lysogenic λ phage strains have different lysis times, ranging from 29.3 min to 68 min, and adsorption rates, spanning from 9.9×10^{-9} to 1.3×10^{-9} $phage^{-1}$ $cell^{-1}$ ml^{-1} min^{-1} (Shao and Wang, 2008). To prevent phage-infected cells from entering the lytic life cycle, the change in cell density of phage P1-infected strains was monitored by measuring OD_{600} at regular time points (Zeng and Golding, 2011). Moreover, to minimize the effect of different growth rates of each strain and ensure total infection by phages, we measured phage titres in cell lysates after incubating the host cells with phage P1 for 15 min. This incubation time is shorter than the average doubling time of *E. coli* and the lysis time of phages, ensuring that the bias caused by differences in the host cell replication rate was minimized. Given that the doubling times of *crp*, *cyaA* and *hns* deletion mutants (44, 45 and 51 min respectively) were slower than those of the wild-type cells (27 min) (D'Ari *et al.*, 1988) (Rouquette *et al.*, 2004), CRISPR deletion mutant cells (26 min), and *cse3* deletion mutant cells (25 min), the bias of the host replication rate cannot be ruled out, even when a short incubation time is used. Therefore, the phages were incubated with the wild-type or mutant strains of *E. coli*, but each PFU was analysed in wild-type strains.

Plasmid stability and plasmid-interfering mutant analysis

The *E. coli* BW25113 transformed with pSB3T5 derivative plasmids (pI3, pP3, pI7 and pP7) was serially diluted and spread on the LB plate containing tetracycline (10 μg ml^{-1}). Single colonies collected from the plate were grown in LB with tetracycline (10 μg ml^{-1}) overnight, after which the culture (50 μl) was placed into a fresh LB medium (5 ml) and grown at 37°C until OD_{600} reached 1.0. Finally, these cultures were serially diluted and plated on LB plate to obtain single colonies. For each culture, 200 colonies were collected and grown on LB plates in the presence or absence of tetracycline. The relative plasmid stability was calculated by comparing the number of colonies on the LB agar plate containing tetracycline (10 μg ml^{-1}) with the number of colonies on pure LB agar.

Bioinformatics analysis

The sequences of all *E. coli* CRISPR spacers were collected from CRISPRdb (Grissa *et al.*, 2007), a database providing the full genome sequences of 48 *E. coli* strains. In 42 of these strains, 688 CRISPR spacers were found. These spacers were matched to the genome sequence of different bacteriophages, including P1(NC_005856.1), P2(NC_001895.1), T4(AF158101.6), T5(NC_005859.1), T7(NC_001604.1), lambda(λ)(NC_001416.1), M13(NC_003287.2), Qβ(NC_001890.1), MS2(NC_001417.2) and ΦX174(NC_001422.1), using the BLASTn program (Altschul *et al.*, 1990; Mount, 2007). All parameters used in BLAST are the same as those in the default setting. Only the matches containing the base-pairing region spanning more than 16 base pairs were considered statistically significant and were reported.

Acknowledgements

We would like to thank Dr Steve Busby of the School of Biosciences, University of Birmingham, for donating the pRW50, pDU9 and pDCRP plasmids. We are also grateful for Enago (http://www.enago.tw) for the English language review. This manuscript was supported by the National Science Council of the Republic of China [Contracts NSC 102-2627-B-009-002, NSC 101-2311-B-009-003-MY3 and NSC 102-2911-I-009-101] and the Veterans General Hospitals and University System of Taiwan (VGHUST) [Grant VGHUST103-G5-1-2].

References

Agari, Y., Sakamoto, K., Tamakoshi, M., Oshima, T., Kuramitsu, S., and Shinkai, A. (2010) Transcription profile of *Thermus thermophilus* CRISPR systems after phage infection. *J Mol Biol* **395:** 270–281.

Aiba, H., Mori, K., Tanaka, M., Ooi, T., Roy, A., and Danchin, A. (1984) The complete nucleotide sequence of the adenylate cyclase gene of *Escherichia coli*. *Nucleic Acids Res* **12:** 9427–9440.

Ali Azam, T., Iwata, A., Nishimura, A., Ueda, S., and Ishihama, A. (1999) Growth phase-dependent variation in protein composition of the *Escherichia coli* nucleoid. *J Bacteriol* **181:** 6361–6370.

Altschul, S.F., Gish, W., Miller, W., Myers, E.W., and Lipman, D.J. (1990) Basic local alignment search tool. *J Mol Biol* **215:** 403–410.

Baba, T., Ara, T., Hasegawa, M., Takai, Y., Okumura, Y.,

Baba, M., *et al*. (2006) Construction of *Escherichia coli* K-12 in-frame, single-gene knockout mutants: the Keio collection. *Mol Syst Biol* **2:** 0008.

Barrangou, R., Fremaux, C., Deveau, H., Richards, M., Boyaval, P., Moineau, S., *et al*. (2007) CRISPR provides acquired resistance against viruses in prokaryotes. *Science* **315:** 1709–1712.

Blaszczyk, U., Polit, A., Guz, A., and Wasylewski, Z. (2001) Interaction of cAMP receptor protein from *Escherichia coli* with cAMP and DNA studied by dynamic light scattering and time-resolved fluorescence anisotropy methods. *J Protein Chem* **20:** 601–610.

Brodersen, P., and Voinnet, O. (2009) Revisiting the principles of microRNA target recognition and mode of action. *Nat Rev Mol Cell Biol* **10:** 141–148.

Brouns, S.J., Jore, M.M., Lundgren, M., Westra, E.R., Slijkhuis, R.J., Snijders, A.P., *et al*. (2008) Small CRISPR RNAs guide antiviral defense in prokaryotes. *Science* **321:** 960–964.

Buettner, M.J., Spitz, E., and Rickenberg, H.V. (1973) Cyclic adenosine 3′,5′-monophosphate in *Escherichia coli*. *J Bacteriol* **114:** 1068–1073.

Chen, Y.P., Lin, H.H., Yang, C.D., Huang, S.H., and Tseng, C.P. (2012) Regulatory role of cAMP receptor protein over *Escherichia coli* fumarase genes. *J Microbiol* **50:** 426–433.

Chng, C., Lum, A.M., Vroom, J.A., and Kao, C.M. (2008) A key developmental regulator controls the synthesis of the antibiotic erythromycin in *Saccharopolyspora erythraea*. *Proc Natl Acad Sci USA* **105:** 11346–11351.

Datsenko, K.A., Pougach, K., Tikhonov, A., Wanner, B.L., Severinov, K., and Semenova, E. (2012) Molecular memory of prior infections activates the CRISPR/Cas adaptive bacterial immunity system. *Nat Commun* **3:** 945.

D'Ari, R., Jaffe, A., Bouloc, P., and Robin, A. (1988) Cyclic AMP and cell division in *Escherichia coli*. *J Bacteriol* **170:** 65–70.

Deveau, H., Garneau, J.E., and Moineau, S. (2010) CRISPR/Cas system and its role in phage-bacteria interactions. *Annu Rev Microbiol* **64:** 475–493.

Diez-Villasenor, C., Almendros, C., Garcia-Martinez, J., and Mojica, F.J. (2010) Diversity of CRISPR loci in *Escherichia coli*. *Microbiology* **156:** 1351–1361.

Ellis, E.L., and Delbruck, M. (1939) The Growth of Bacteriophage. *J Gen Physiol* **22:** 365–384.

Fang, M., Majumder, A., Tsai, K.J., and Wu, H.Y. (2000) ppGpp-dependent leuO expression in bacteria under stress. *Biochem Biophys Res Commun* **276:** 64–70.

Garneau, J.E., Dupuis, M.E., Villion, M., Romero, D.A., Barrangou, R., Boyaval, P., *et al*. (2010) The CRISPR/Cas bacterial immune system cleaves bacteriophage and plasmid DNA. *Nature* **468:** 67–71.

Gaudreault, M., Gingras, M.E., Lessard, M., Leclerc, S., and Guerin, S.L. (2009) Electrophoretic mobility shift assays for the analysis of DNA-protein interactions. *Methods Mol Biol* **543:** 15–35.

Gorke, B., and Stulke, J. (2008) Carbon catabolite repression in bacteria: many ways to make the most out of nutrients. *Nat Rev Microbiol* **6:** 613–624.

Grissa, I., Vergnaud, G., and Pourcel, C. (2007) The CRISPRdb database and tools to display CRISPRs and to generate dictionaries of spacers and repeats. *BMC Bioinformatics* **8:** 172.

Haft, D.H., Selengut, J., Mongodin, E.F., and Nelson, K.E. (2005) A guild of 45 CRISPR-associated (Cas) protein families and multiple CRISPR/Cas subtypes exist in prokaryotic genomes. *PLoS Comput Biolog* **1:** e60.

Hale, C., Kleppe, K., Terns, R.M., and Terns, M.P. (2008) Prokaryotic silencing (psi)RNAs in *Pyrococcus* furiosus. *RNA* **14:** 2572–2579.

Harman, J.G. (2001) Allosteric regulation of the cAMP receptor protein. *Biochim Biophys Acta* **1547:** 1–17.

Henikoff, S., Haughn, G.W., Calvo, J.M., and Wallace, J.C. (1988) A large family of bacterial activator proteins. *Proc Natl Acad Sci USA* **85:** 6602–6606.

Hollands, K., Busby, S.J., and Lloyd, G.S. (2007) New targets for the cyclic AMP receptor protein in the *Escherichia coli* K-12 genome. *FEMS Microbiol Lett* **274:** 89–94.

Howard, J.A., Delmas, S., Ivancic-Bace, I., and Bolt, E.L. (2011) Helicase dissociation and annealing of RNA-DNA hybrids by *Escherichia coli* Cas3 protein. *Biochem J* **439:** 85–95.

Johansson, J., Balsalobre, C., Wang, S.Y., Urbonaviciene, J., Jin, D.J., Sonden, B., and Uhlin, B.E. (2000) Nucleoid proteins stimulate stringently controlled bacterial promoters: a link between the cAMP-CRP and the (p)ppGpp regulons in *Escherichia coli*. *Cell* **102:** 475–485.

Jore, M.M., Lundgren, M., van Duijn, E., Bultema, J.B., Westra, E.R., Waghmare, S.P., *et al*. (2011) Structural basis for CRISPR RNA-guided DNA recognition by Cascade. *Nat Struct Mol Biol* **18:** 529–536.

Karr, E.A. (2010) The methanogen-specific transcription factor MsvR regulates the *fpaA-rlp-rub* oxidative stress operon adjacent to *msvR* in *Methanothermobacter thermautotrophicus*. *J Bacteriol* **192:** 5914–5922.

Keseler, I.M., Mackie, A., Peralta-Gil, M., Santos-Zavaleta, A., Gama-Castro, S., Bonavides-Martinez, C., *et al*. (2013) EcoCyc: fusing model organism databases with systems biology. *Nucleic Acids Res* **41:** D605–D612.

Kolb, A., Busby, S., Buc, H., Garges, S., and Adhya, S. (1993) Transcriptional regulation by cAMP and its receptor protein. *Annu Rev Biochem* **62:** 749–795.

Lawson, C.L., Swigon, D., Murakami, K.S., Darst, S.A., Berman, H.M., and Ebright, R.H. (2004) Catabolite activator protein: DNA binding and transcription activation. *Curr Opin Struct Biol* **14:** 10–20.

Lin, H.H., Hsu, C.C., Yang, C.D., Ju, Y.W., Chen, Y.P., and Tseng, C.P. (2011) Negative effect of glucose on *ompA* mRNA Stability: a potential role of cyclic AMP in the repression of *hfq* in *Escherichia coli*. *J Bacteriol* **193:** 5833–5840.

Lobocka, M.B., Rose, D.J., Plunkett, G., 3rd, Rusin, M., Samojedny, A., Lehnherr, H., *et al*. (2004) Genome of bacteriophage P1. *J Bacteriol* **186:** 7032–7068.

Lorenz, R., I., Hofacker, L., and Bernhart, S.H. (2012) Folding RNA/DNA hybrid duplexes. *Bioinformatics* **28:** 2530–2531.

Majumder, A., Fang, M., Tsai, K.J., Ueguchi, C., Mizuno, T., and Wu, H.Y. (2001) LeuO expression in response to starvation for branched-chain amino acids. *J Biol Chem* **276:** 19046–19051.

Makarova, K.S., Haft, D.H., Barrangou, R., Brouns, S.J., Charpentier, E., Horvath, P., *et al*. (2011) Evolution and classification of the CRISPR-Cas systems. *Nat Rev Microbiol* **9:** 467–477.

Marraffini, L.A., and Sontheimer, E.J. (2010) CRISPR inter-

ference: RNA-directed adaptive immunity in bacteria and archaea. *Nat Rev Genet* **11:** 181–190.
Minetti, C.A., Remeta, D.P., Dickstein, R., and Breslauer, K.J. (2010) Energetic signatures of single base bulges: thermodynamic consequences and biological implications. *Nucleic Acids Res* **38:** 97–116.
Mojica, F.J., Diez-Villasenor, C., Garcia-Martinez, J., and Almendros, C. (2009) Short motif sequences determine the targets of the prokaryotic CRISPR defence system. *Microbiology* **155:** 733–740.
Mount, D.W. (2007) Using the Basic Local Alignment Search Tool (BLAST). *CSH Protoc* **2007:** pdb top17.
Paez-Espino, D., Morovic, W., Sun, C.L., Thomas, B.C., Ueda, K., Stahl, B., *et al*. (2013) Strong bias in the bacterial CRISPR elements that confer immunity to phage. *Nat Commun* **4:** 1430.
Poranen, M.M., Ravantti, J.J., Grahn, A.M., Gupta, R., Auvinen, P., and Bamford, D.H. (2006) Global changes in cellular gene expression during bacteriophage PRD1 infection. *J Virol* **80:** 8081–8088.
Pougach, K., Semenova, E., Bogdanova, E., Datsenko, K.A., Djordjevic, M., Wanner, B.L., and Severinov, K. (2010) Transcription, processing and function of CRISPR cassettes in *Escherichia coli*. *Mol Microbiol* **77:** 1367–1379.
Pul, U., Wurm, R., Arslan, Z., Geissen, R., Hofmann, N., and Wagner, R. (2010) Identification and characterization of *E. coli* CRISPR-cas promoters and their silencing by H-NS. *Mol Microbiol* **75:** 1495–1512.
Rouquette, C., Serre, M.C., and Lane, D. (2004) Protective role for H-NS protein in IS1 transposition. *J Bacteriol* **186:** 2091–2098.
Saxena, S., Jonsson, Z.O., and Dutta, A. (2003) Small RNAs with imperfect match to endogenous mRNA repress translation. Implications for off-target activity of small inhibitory RNA in mammalian cells. *J Biol Chem* **278:** 44312–44319.
Semenova, E., Jore, M.M., Datsenko, K.A., Semenova, A., Westra, E.R., Wanner, B., *et al*. (2011) Interference by clustered regularly interspaced short palindromic repeat (CRISPR) RNA is governed by a seed sequence. *Proc Natl Acad Sci USA* **108:** 10098–10103.
Shao, Y., and Wang, I.N. (2008) Bacteriophage adsorption rate and optimal lysis time. *Genetics* **180:** 471–482.
Shetty, R.P., Endy, D., and Knight, T.F., Jr (2008) Engineering BioBrick vectors from BioBrick parts. *J Biol Eng* **2:** 5.
Smith, A.L., Cekan, P., Brewood, G.P., Okonogi, T.M., Alemayehu, S., Hustedt, E.J., *et al*. (2009) Conformational equilibria of bulged sites in duplex DNA studied by EPR spectroscopy. *J Phys Chem B* **113:** 2664–2675.
Stern, A., and Sorek, R. (2011) The phage-host arms race: shaping the evolution of microbes. *Bioessays* **33:** 43–51.
Thattai, M., and Shraiman, B.I. (2003) Metabolic switching in the sugar phosphotransferase system of *Escherichia coli*. *Biophys J* **85:** 744–754.
Touchon, M., Charpentier, S., Clermont, O., Rocha, E.P., Denamur, E., and Branger, C. (2011) CRISPR distribution within the *Escherichia coli* species is not suggestive of immunity-associated diversifying selection. *J Bacteriol* **193:** 2460–2467.
Ueguchi, C., Ohta, T., Seto, C., Suzuki, T., and Mizuno, T. (1998) The leuO gene product has a latent ability to relieve bgl silencing in *Escherichia coli*. *J Bacteriol* **180:** 190–193.
Westra, E.R., and Brouns, S.J. (2012) The rise and fall of CRISPRs–dynamics of spacer acquisition and loss. *Mol Microbiol* **85:** 1021–1025.
Westra, E.R., Pul, U., Heidrich, N., Jore, M.M., Lundgren, M., Stratmann, T., *et al*. (2010) H-NS-mediated repression of CRISPR-based immunity in *Escherichia coli* K12 can be relieved by the transcription activator LeuO. *Mol Microbiol* **77:** 1380–1393.
Westra, E.R., van Erp, P.B., Kunne, T., Wong, S.P., Staals, R.H., Seegers, C.L., *et al*. (2012) CRISPR immunity relies on the consecutive binding and degradation of negatively supercoiled invader DNA by Cascade and Cas3. *Mol Cell* **46:** 595–605.
Westra, E.R., Semenova, E., Datsenko, K.A., Jackson, R.N., Wiedenheft, B., Severinov, K., and Brouns, S.J. (2013) Type I-E CRISPR-cas systems discriminate target from non-target DNA through base pairing-independent PAM recognition. *PLoS Genet* **9:** e1003742.
Wiedenheft, B., Lander, G.C., Zhou, K., Jore, M.M., Brouns, S.J., van der Oost, J., *et al*. (2011) Structures of the RNA-guided surveillance complex from a bacterial immune system. *Nature* **477:** 486–489.
Wiedenheft, B., Sternberg, S.H., and Doudna, J.A. (2012) RNA-guided genetic silencing systems in bacteria and archaea. *Nature* **482:** 331–338.
Won, H.S., Lee, T.W., Park, S.H., and Lee, B.J. (2002) Stoichiometry and structural effect of the cyclic nucleotide binding to cyclic AMP receptor protein. *J Biol Chem* **277:** 11450–11455.
Yosef, I., Goren, M.G., and Qimron, U. (2012) Proteins and DNA elements essential for the CRISPR adaptation process in *Escherichia coli*. *Nucleic Acids Res* **40:** 5569–5576.
Zeng, L., and Golding, I. (2011) Following cell-fate in *E. coli* after infection by phage lambda. *J Vis Exp* **56:** e3363.
Zianni, M., Tessanne, K., Merighi, M., Laguna, R., and Tabita, F.R. (2006) Identification of the DNA bases of a DNase I footprint by the use of dye primer sequencing on an automated capillary DNA analysis instrument. *J Biomol Tech* **17:** 103–113.

Supporting information

Additional supporting information may be found in the online version of this article at the publisher's web-site.